Summer 2016

Seagrasses (Zostera marina) and (Zostera japonica) Display a Differential Photosynthetic Response to TCO2: Implications for Acidification Mitigation

Cale A. Miller
Western Washington University, calemiller620@gmail.com

SEAGRASSES (ZOSTERA MARINA) AND (ZOSTERA JAPONICA) DISPLAY A DIFFERENTIAL PHOTOSYNTHETIC RESPONSE TO TCO_2: IMPLICATIONS FOR ACIDIFICATION MITIGATION

By

Cale A. Miller

Accepted in Partial Completion
Of the Requirements for the Degree
Master of Science

Kathleen Kitto, Dean of the Graduate School

ADVISORY COMMITTEE

Chair, Dr. Brooke Love

Dr. Sylvia Yang

Dr. David Shull

MASTER'S THESIS

In presenting this thesis in partial fulfillment of the requirements for a master's degree at Western Washington University, I grant to Western Washington University the non-exclusive royalty-free right to archive, reproduce, distribute, and display the thesis in any and all forms, including electronic format, via any digital library mechanisms maintained by WWU.

I represent and warrant this is my original work, and does not infringe or violate any rights of others. I warrant that I have obtained written permissions from the owner of any third party copyrighted material included in these files.

I acknowledge that I retain ownership rights to the copyright of this work, including but not limited to the right to use all or part of this work in future works, such as articles or books.

Library users are granted permission for individual, research and non-commercial reproduction of this work for educational purposes only. Any further digital posting of this document requires specific permission from the author.

Any copying or publication of this thesis for commercial purposes, or for financial gain, is not allowed without my written permission.

Cale Miller
July 15, 2016

SEAGRASSES (ZOSTERA MARINA) AND (ZOSTERA JAPONICA) DISPLAY A DIFFERENTIAL PHOTOSYNTHETIC RESPONSE TO TCO_2: IMPLICATIONS FOR ACIDIFICATION MITIGATION

A thesis Presented to
The Faculty of
Western Washington University

Accepted in Partial Completion
Of the Requirements for the Degree
Master of Science

by

Cale A. Miller

August 2015

Abstract

Excess atmospheric CO_2 is being absorbed at an unprecedented rate by the global and coastal oceans, shifting the baseline pCO_2 and altering seawater carbonate chemistry in a process known as ocean acidification (OA). Recent attention has been given to near-shore vegetated habitats, such as seagrass beds, which may have the potential to mitigate the effects of acidification on vulnerable calcifying organisms via photosynthesis. Seagrasses are capable of raising seawater pH and calcium carbonate saturation state during times of high photosynthetic activity. To better understand the photosynthetic potential of seagrass OA mitigation, we exposed Pacific Northwest populations of native *Zostera marina* and non-native *Zostera japonica* seagrasses from Padilla Bay, WA, to various irradiance and total CO_2 (TCO_2) concentrations ranging from ~1770 – 2100 μmol TCO_2 kg^{-1}.

Our results indicate that the maximum net photosynthetic rate (P_{max}) for *Z. japonica* as a function of irradiance and TCO_2 was 3x greater than *Z. marina* when standardized to chlorophyll (360 ± 74 μmol TCO_2 mg chl^{-1} hr^{-1} and 113 ± 21 μmol TCO_2 mg chl^{-1} hr^{-1}, respectively). In addition, *Z. japonica* increased its P_{max} 77% (± 56%) when TCO_2 increased from ~1770 to 2050 μmol TCO_2 kg^{-1}, whereas *Z. marina* did not display an increase in P_{max} with higher TCO_2. The lack of response by *Z. marina* to TCO_2 is a departure from previous findings; however, it is likely that the variance within our treatments (coefficient of variation: 30 – 60%) obscured any positive effect of TCO_2 on *Z. marina* given the range of concentrations tested. Because previous findings have shown that *Z. marina* is saturated with respect to HCO_3^- at low pH (≥ 7.5) we, therefore, suggest that the unequivocal positive response of *Z. japonica* to TCO_2 is a result of increased HCO_3^- utilization in addition to increased CO_2 uptake.

Considering that *Z. japonica* displays a greater photosynthetic rate than *Z. marina* when normalized to chlorophyll, particularly under enhanced TCO_2 conditions, the ability of *Z. japonica* to mitigate OA may also increase relative to *Z. marina* in the future ocean. Higher photosynthetic rates by *Z. japonica* result in a greater potential, on a per chlorophyll basis, to increase pH and calcium carbonate saturation state—both of which affect acid-base regulation and calcification of calcifying organisms vulnerable to acidification. While it is important to consider genotypic differences throughout *Z. marina* and *Z. japonica*'s biogeographical distribution, our findings help elucidate the potential contribution both seagrasses have on variations in carbonate chemistry. Further, our results could be applied to ecosystem service models aimed at determining how specific seagrass species can be grown in a controlled setting to help mitigate OA hotspots that affect commercial shellfish aquaculture.

Acknowledgements

I would like to express my gratitude to the Padilla Bay Foundation, Dr. Jude Apple, and Sharon Riggs who supported this research and granted financial assistance for the work. I would also like to thank Huxley College for providing financial assistance to conduct this research and assist with travel expenses to present my work nationally and internationally.

First, I acknowledge my graduate advisor, Dr. Brooke Love, for her support and expertise in oceanography and seawater chemistry. She provided me with great independence when conducting my research, which allowed me to be creative and work through problems, all the while being readily available to assist with questions and solutions to problems. I would also like to thank my committee members Dr. Sylvia Yang and Dr. David Shull, who provided their expertise in seagrass biology and analytical methodologies. I acknowledge Dr. Katherina Schoo for sharing her skills and knowledge in the operation of instruments used to measure carbonate chemistry.

I extend a great thanks to my fellow graduate students Rachel Blyth, Melissa Ciesielski, Taylor Clement, Rosie Gradoville, and Anne Harmann who were integral for carrying out the experiments. They provided needed friendship and support during my time at WWU.

Table of Contents

List of Figures

List of Tables

Introduction

The rate at which anthropogenic fossil fuel emissions are taken up by the global oceans is shifting the acid-base balance of the oceanic carbonate system, leading to a decrease in carbonate mineral saturation state ($\Omega_{ar/cal}$) and pH, in a process known as ocean acidification (OA) (Sabine et al. 2004, Orr et al. 2005, Hönisch et al. 2012). While an increasing baseline of CO_2 will affect the entirety seawater carbonate chemistry, coastal ocean carbonate chemistry is predominately driven by biological metabolism, riverine discharge and associated organic matter composition, tidal pumping, upwelling, nutrient input, and eutrophication (Feely et al. 2008, Cai 2011, Duarte et al. 2013, Waldbusser and Salisbury 2014, Wallace et al. 2014). These myriad factors driving coastal ocean carbonate chemistry induce high variability to the system, and result in periodic and episodic pH and saturation state decreases that are more extreme than the ~0.4 pH and ~1.5 Ω_{ar} decreases that are predicted for in open ocean surface waters by the end of the century (Duarte et al. 2013, Ciais et al. 2014, Waldbusser and Salisbury 2014). The high variability of coastal ocean carbonate chemistry is expected to be superimposed on the long term global trend of increasing seawater CO_2, potentially leading to even more extreme conditions for near-shore coastal waters (Harris et al. 2013, Hauri et al. 2013, Waldbusser and Salisbury 2014). It is possible, however, that biological photosynthetic and respiration cycles, which in large part control coastal ocean carbonate chemistry, may respond in a way that could dampen or exacerbate the magnitude of extreme carbonate chemistry events. Due to the economic and social vulnerability of human coastal communities to near-shore acidification (Ekstrom et al. 2015), it is imperative to understand how coastal acidification may be mitigated on a local scale in order to prevent the negative effects on ecologically important organisms and ecosystems.

A broad range of organisms will exhibit impaired survival, growth, and calcification from the effects of acidification—increasing the potential for shifts in ecosystem dynamics by altering species distribution, diversity, and organismal competitive interactions (Doney et al. 2009, Kroeker et al. 2010, 2013, Gaylord et al. 2015). Due to the natural variability of the carbonate system in near-shore coastal waters, however, it has been suggested that resident calcifying organisms vulnerable to the effects of acidification may be more physiologically resilient if they demonstrate plasticity and are pre-adapted to highly variable carbonate systems (Pörnter 2008, Hofmann et al. 2011, Bernhardt and Leslie 2013). While some organisms may indeed demonstrate an increased tolerance to highly variably carbonate chemistry, it is important to recognize species-specific resilience to acidification. For example, a recent study comparing the effects of acidification on larval mussels found there to be no difference in development and growth between mussels pre-adapted to areas that experience season upwelling—and therefore high spatial and temporal carbonate chemistry variability— and those local to an area without upwelling (Waldbusser et al. 2015a).

While many calcifying organisms will be negatively affected by acidification, some autotrophs may benefit from rising concentrations of seawater CO_2 by increasing photosynthesis and growth (Kroeker et al. 2010, 2013, Koch et al. 2013). The positive effects of increasing CO_2 on organisms such as macrophytes have spurred research investigating the potential mitigating effects of seagrass photosynthesis on acidification (Unsworth et al. 2012, Manzello et al. 2012, Hendriks et al. 2014). OA mitigation by seagrass specifically refers to the removal of CO_2 from seawater, which raises the pH and reduces the TCO_2 (i.e., sum of all forms of carbonic acid and its conjugate bases), minimizing unfavorable carbonate chemistry prevalence (Marbà 2006, Unsworth et al. 2012). The premise of seagrass as OA refuge originates from evidence indicating

that in near-shore, shallow coastal waters, most seagrass systems tend to be net autotrophic, sequestering large amounts carbon (Duarte et al. 2010, 2011, Unsworth et al. 2012). Net autotrophic seagrass systems, however, foster enhanced rates of respiration, due to the accumulation of allochthonous organic matter within their canopies, and from dark respiration by seagrass themselves; this results in a biologically dominated carbonate system with high variability on a diurnal scale (Koch et al. 2006, Duarte et al. 2013, Hendriks et al. 2014, Waldbusser and Salisbury 2014, Wallace et al. 2015).

Three different mechanisms, or a combination of, appear to act as the primary means for TCO_2 uptake: direct CO_2 uptake from the DBL, carbonic anhydrase (CA) secretion in to the cell wall which dehydrates bicarbonate ($HCO_3^- + CA \rightarrow CO_2$), and symport of HCO_3^- via proton pumping (Beer et al. 2002, Larkum 2006, Koch et al. 2013). In addition, studies have found that increases in seawater TCO_2 can enhance seagrass photosynthesis, growth, biomass, and tissue thickness (Beer and Koch 1996, Thom 1996, Zimmerman 1997, Kroeker et al. 2013, Koch et al. 2013, Cox et al. 2016). These findings are not universal, however, and the capacity of TCO_2 uptake by seagrass varies by species, geographical location, distribution depth, and the process by which TCO_2 moves across the diffusive boundary layer (DBL) and cell wall (Larkum 2006, Lee et al. 2007, Koch et al. 2013). Due to species-specific physiology, the full potential and ability to uptake TCO_2 varies, as evidence shows mixed results of HCO_3^- saturation points and changes in photosynthetic rate when exposed to high TCO_2 levels under replete and limited light intensities (Beer and Koch 1996, Zimmerman et al. 1997, Palacios and Zimmerman 2007, Invers et al. 2001, Ow et al. 2016, Cox et al. 2016). Even though ambiguity remains regarding the mechanisms and degree of TCO_2 uptake, studies have determined that most seagrass species are carbon limited at present day TCO_2 levels (Larkum 2006 and references therein, Koch et al.

2013, Hendriks et al. 2014). The apparent TCO_2 limitation of seagrasses, therefore, has implications for how individual species will respond to a globally increasing TCO_2 baseline, which will likely alter the photosynthetic potential, and affect the amelioration of OA by seagrasses.

Numerous studies have examined the long-term carbon sequestration potential of seagrass beds (Duarte et al. 2005, 2011, Chung et al. 2011, McLeod et al. 2011, Fourqurean et al. 2012, Marbà et al. 2015, Poppe 2015). While burial determines long-term effects of seagrass on carbon cycling, it does not drive OA-mitigation potential on short timescales; rather, instantaneous photosynthetic rates are more relevant. Short-term carbon drawdown on the hourly scale coincides with timescales of rapid development for calcifiers, for whom sensitivity to OA is driven by the duration and intensity of exposure (Kurihara 2008, Talmage and Gobler 2009, Hettinger et al. 2012, Waldbusser et al. 2015b). The continued uptake of CO_2 by surface waters will increase the baseline CO_2 affecting the frequency, duration, and magnitude of acidification events in coastal waters (Harris et al. 2013, Hauri et al. 2013, Waldbusser and Salisbury 2014). That is, increasing the duration and magnitude of carbonate chemistry variability will likely result in conditions that periodically surpass physiological thresholds of resident organisms that already exist at their tolerance limits (Grantham et al. 2004, Waldbusser and Salisbury 2014). Seagrasses, however, may be able to improve times of favorable carbonate chemistry, or dampen episodic extremes of unfavorable carbonate chemistry on hourly timescales, thus lessening the duration and magnitude of exposure to extreme acidification.

In the U.S. Pacific Northwest (PNW) where OA mitigation initiatives have been established for the Salish Sea, seagrasses have been specifically identified as a biological means to offset the effects of acidification (Blue Ribbon Panel on Ocean Acidification 2012). Two

seagrass species found in the Salish Sea: native *Zostera marina* L. and non-native *Zostera japonica* Ascher. & Graeb. have strong habitat-association with organisms vulnerable to OA (Harrison 1982a, Ferraro and Cole. 2012, Mach et al. 2014, Dumbauld and McCoy 2015). Whereas *Z. marina* has been the focus of many studies examining its high photosynthetic rate (Lee et al. 2007) and response to TCO_2 increase (Beer and Koch 1996, Thom 1996, Zimmerman et al. 1997, Koch et al. 2013), little work has been done investigating *Z. japonica* photosynthesis and physiology for established PNW populations (Shafer et al. 2011, Shafer and Kaldy 2014, Kaldy et al. 2015). In the Salish Sea, *Z. japonica* occurs in the mid to upper intertidal zone where it has transformed previously unvegetated mudflats via continued expansion of its distribution, and has thus been labeled as a noxious weed in Washington state (NWCB 2012, Thom et al. 2014). Conversely, *Z. marina* is a protected species with a distribution extending from the lower intertidal to shallow subtidal region: species overlap with *Z. japonica* can occur in the lower intertidal zone on flat shorelines (Harrison 1982a, Thom 1990, Ruesink et al. 2010, Thom et al. 2014). Despite *Z. japonica*'s designation as a noxious weed in Washington state, studies have highlighted that the non-native seagrass provides many of the benefits associated with other seagrasses, including predator protection, sediment stability, and enhanced community productivity and diversity (Orth et al. 1984, Duffy 2006, Wonham and Carlton 2005, Mach et al. 2014). Given the potential of *Z. japonica* to colonize unvegetated habitat and, thus, increase the expanse of seagrass meadows, it is relevant to consider how the photosynthetic potential of *Z. japonica*—in addition to *Z. marina*—impacts and interacts with the carbonate system, given that seagrass OA mitigation is a focus in the Salish Sea (Blue ribbon panel on ocean acidification 2012)

To better understand how *Z. marina* and *Z. japonica* may mitigate the effects of acidification, studies investigating the photosynthetic potential and efficiency in response to TCO_2 increase are needed. A recent study comparing *Z. marina* and *Z. japonica* photosynthesis found that *Z. japonica* has a higher photosynthetic rate; however, the results are specific to populations on the central Oregon coast (Shafer and Kaldy 2014), and geographical location most be considered as local adaptations exists throughout a species' distribution (Backman 1991 and references therein). Given the importance of site-specific physiology, we investigated the differential responses of photosynthetic rates over a spectrum of irradiance and seawater TCO_2. Specifically, we conducted one experiment per species to examine the (1) potential differences in photosynthetic rates between *Z. marina* and *Z. japonica,* (2) how changes in TCO_2 affect photosynthetic rates, and (3) how the photosynthetic potential is likely to induce hourly changes on the carbonate system.

Methods

Sample Site and collection. Padilla Bay, Washington, is a tidally dominated estuary in the Salish Sea, and is a part of the National Estuarine Research Reserve System (48° 31' 14.1" N, 122° 35' 24.4" W). The *Z. marina* and *Z. japonica* beds in Padilla Bay are considered to be one of the most contiguous stands on the North American Pacific Coast, constituting a submerged and emergent total area of ~4,000 ha, where *Z. marina* accounts for ~3,000 of the total area (Bulthuis 2013). In the lower intertidal region where *Z. japonica* distribution diminishes and transitions to *Z. marina* moving offshore, the morphological difference of *Z. japonica* is conspicuous, with a surface area and mass that is ~5x less than that of *Z. marina* when comparing equal length segments. In the lower intertidal where species overlap occurs, a 250 m

transect was marked for shoot collection two weeks prior to sampling. (48° 29' 36.6" N, 122° 29' 8.5" W). Two HOBO Pendant Temperature/Light 64k data loggers were attached ~1 m above the sediment on transect marking poles for the purpose of obtaining irradiance data at the elevations where *Z. japonica* and *Z. marina* co-occur (average tidal height of two consecutive sunny days used in analysis ranged from -0.55 – 3.0 m MLLW). Light sensors logged irradiance for ~12 days before they were collected from the field.

Healthy-looking adult *Z. marina* shoots with intact rhizomes were collected by hand during low tide (0.8 m MLLW) on August 16, 2015 from Padilla Bay along the entire 250 m transect. Ten days later (2nd experiment) on August 26, 2015, adult *Z. japonica* shoots with intact rhizomes were collected in the same manner at low tide (~0.0 MLLW). Approximately 200 shoots of each species were collected, placed in a cooler, and transported to Shannon Point Marine Center in Anacortes, Washington, within 1 hour of collection. One hundred of the most healthy looking 200 shoots (i.e., shoots without visible damage and well preserved rhizomes) were then haphazardly selected, rinsed with seawater, and dispersed among four separate 40-liter acrylic flow through tanks under low irradiance (~50 umol photons m^{-2} s^{1}) on a 12:12 L:D cycle for ~48 hours before experimentation. The 48 hour holding period also served the purpose of acclimating shoots to a slightly higher salinity than found at collection site: ~28 – 29 PSU.

Experimental system. A light fixture housing five T5 high output 54W 6500K Spectralux bulbs was mounted to the bottom of a box with one open side, and was used as the experimental chamber for both experiments. A 5/8" clear acrylic sheet covered the top of the light fixture. Five, shallow, three-sided clear acrylic boxes (56.5 x 7.62 x 3.81 cm) fitted with flow through seawater taps were mounted to the acrylic sheet and placed directly above an individual bulb in

the fixture. Shallow acrylic boxes served as water baths to stabilize temperature, and as position holders for incubating vials (Fig. 1). 20 ml borosilicate scintillation vials with a polyethylene cone-shaped liner were used as incubation vessels, and were nearly fully submerged (water line stopped at cap) when placed in acrylic water baths. Vinyl mesh wraps were constructed and fitted to scintillation vials to attenuate light. Mesh covers either had one, three, or six layers, which provided an irradiance range from ~40 – 500 μmol photons m^{-2} s^{-1}.

Seawater pumped from Guemes Channel was collected, 0.2 μm filtered, sterilized via autoclave, and distributed into five, 20 L polycarbonate carboys. To manipulate CO_2, carboys were fitted with custom plumbed lids for gas exchange, and bubbled with a controlled (Sierra SmartTrak mass flow controller) mixture of compressed ambient air stripped of CO_2 using a regenerative molecular sieve adsorber (Twin Tower Engineering, CAS2-11), and research grade-5 pure CO_2 gas for ~72 hours before use. Carboys were held in an incubator which maintained water temperature at approximately ambient in Guemes Channel: 12.5°C. One liter Nalgene bottles half-way filled with tap water acted as humidifiers, which were plumbed in between gas lines and carboys to minimize the evaporation that occurs when the compressed, dry, and stripped CO_2 air is streamed through the system.

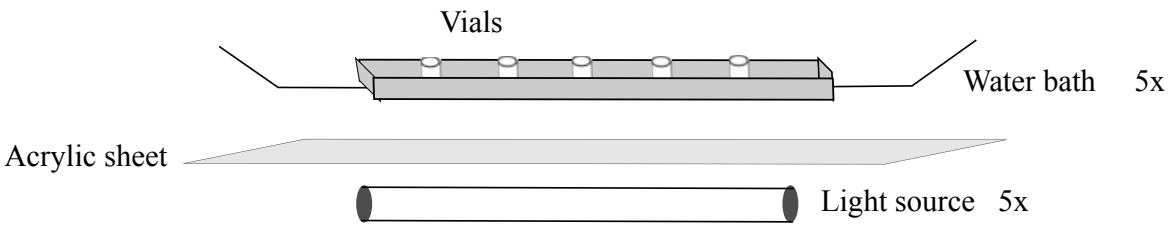

Figure 1. Experimental setup. Light bulbs illuminate from under clear acrylic sheet. Five clear acrylic trays with flow through seawater taps served as water baths that housed experimental vials. Total of 150 vials per experiment: 5 light and 5 pCO_2 conditions yield 25 treatments.

Experimental Design. Leaf segments harvested from shoots served as the experimental unit for both experiments. Approximately 20 hours before experimentation, the middle section of the second youngest leaf in a shoot was selected, wiped clean of epiphytes, and a 2 cm segment for *Z. marina* and 4 cm segment for *Z. japonica* was excised. It should be noted that while the middle section of the leaf was selected for, variation among shoots regarding the overall length of the 2nd youngest leaf existed. Each segment was then cut in half with one segment frozen for chlorophyll extraction, and the other placed into a 20 ml scintillation vial filled with 5 ml of filtered and sterilized seawater. Leaf segment stocked vials were then held in an incubator at 12°C until experimentation.

We used a 5 x 5 factorial design that targeted 25 treatment combinations with an estimated irradiance and pCO_2 range of ~750, 500, 200, 40, 0 μmol photons m^{-2} s^{-1} and ~100, 250, 400, 650, and 900 μatm, respectively. Experimental design consisted of quadruplicate replication and duplicate blanks. Blanks mimicked experimental conditions but lacked leaf segments, and were used to account for any changes in seawater chemistry induced by microbial activity that may have remained after filtration and sterilization. The design resulted in a total of 100 leaf segments and 50 blanks per experiment. Light intensities for treatment values were based on deployed HOBO light pendants at marked transect, and pCO_2 values were selected given the *in situ* variability of the carbonate system in Padilla Bay (Love et al. 2016).

Immediately before each experiment, stocked vials were emptied of filtered seawater, rinsed and filled with treatment seawater. Vials were overflowed to eliminate headspace, and a 0.5-mm glass bead was placed in each vial for the purpose of stirring the seawater. Filled and stocked vials were pre-assigned mesh coverings (no mesh, 1 layer, 3 layer, 6 layer, or opaque) to achieve desired irradiance levels for each leaf segment. Vials were haphazardly placed into water

baths inside lit experimental chamber and incubated for 90 minutes until termination of experiment began. Vials were physically inverted by hand, three times, every five minutes to stir water inside and prevent an oxygen rich and TCO_2 poor boundary layer around leaf segments. Photographs of all vials during the experiment where taken in order to identify the exact position and irradiance emitted at a given spot—irradiance measurements were then taken after the experiment by placing treatment vials back in water baths at their respective locations. Irradiance was measured at each vial location with a QSL-101 PAR irradiance sensor (Biospherical Instruments Inc.).

Photosynthetic measurements. Photosynthetic rates as a function of irradiance and seawater pCO_2 were determined by incubating excised leaf segments of *Z. marina* and *Z. japonica* and measuring seawater TCO_2 before and after incubation. During incubation, temperature in water baths was continuously monitored and recorded every 20 minutes with a Fluke 1523 reference thermometer and probe. Initial conditions of carbonate chemistry were determined for each pCO_2 treatment by collecting triplicate 350 ml total alkalinity (TA) samples in amber glass bottles with polyurethane-lined crimp-sealed metal caps, and triplicate 20 ml samples in scintillation vials for TCO_2 concentration from treatment seawater held in the 20 L carboys (Table 1). All initial condition TCO_2 and TA samples were measured for temperature and salinity (measured with refractometer), poisoned with either 30 or 10 µl of $HgCl_2$ (TA or TCO_2), capped, wrapped with parafilm to minimize any potential gas leakage, and refrigerated at 2°C until analysis. Salinity ranged from 30.5 – 32 $^0/_{00}$ for the *Z. japonica* experiment (Table 1). The variation was likely a result of unequal effectiveness by the humidifiers during bubbling, or

from differential evaporation in autoclaved bottles used to fill carboys, thus resulting in dissimilar evaporation rates in each of the carboys.

To terminate the experiment, vials were removed one at time haphazardly across treatments, but ordinally by replicate assignment—this allowed for an equal experimental termination time across treatments. Each leaf segment was removed from a vial, marked for incubation time, and stored in an empty vial for later dry-weight measurement. The experimental vial was immediately poisoned with 10 µl of a saturated $HgCl_2$ solvent, capped, wrapped with parafilm, and refrigerated at 2°C.

All TCO_2 samples were analyzed within 5 days of each experiment. TCO_2 for each sample was quantified using an Apollo SciTech AS-C3 dissolved inorganic carbon (DIC) analyzer by drawing 0.75 ml samples from the 20 ml scintillation vial 3 – 5 times until two consecutive measurements with a difference no greater than 5 µmol kg^{-1} was measured. TA samples were titrated within 30 days of experiment using the open-cell method as in Dickson et al. (2007) with a Metrohm 888 Titrando. Certified reference material for both TCO_2 and TA analyses was used to construct a five-point standardization curve and verify accuracy of open-cell titration, respectively (Batch 144, A.G., Dickson, Scripps Institute of Oceanography). The partial pressure of CO_2 (µatm) and associated carbonate system parameters pH (total) and aragonite saturation state (Ω_{ar}) were calculated using CO2SYS (Pierrot et al. 2006) with K_1 and K_2 equilibrium constants from Mehrbach et al. (1973) and refit by Dickson and Millero (1987).

Leaf segments from the experiment were rinsed 3x with deionized water and dried at 55°C for at least 24 hours before dry mass was recorded. Frozen leaf segments were prepped for chlorophyll extraction by sonicating for 30 seconds in a 10 ml 90% acetone solution. Segments were then refrozen at -20°C for 24 hrs. and centrifuged for five minutes directly before

chlorophyll measurement. Extract was measured with a Trilogy fluorometer (Turner designs), acidified with 0.1 N HCl, and measured again. Chlorophyll and phaeopigment concentrations were calculated following the methods described by Lorenzen (1966).

Statistical methods and photosynthetic response. Photosynthetic rate as a function of irradiance (*P* vs. *E*) was normalized to chlorophyll (a/b) to minimize variance in photosynthetic pigment content between shoots. *P* vs. *E* curves were fit and photosynthetic parameters estimated using the non-linear hyperbolic tangent function described by Jassby and Platt (1976):

$$P = P_{max} \tanh\left(\frac{\alpha I}{P_{max}}\right) + R_d \quad (1)$$

where P_{max} is the maximum photosynthetic rate (μmol TCO_2 mg chl^{-1} hr^{-1}), I is the irradiance (μmol photons m^{-2} s^{-1}), R_d is the dark respiration rate, and α (photosynthetic efficiency) is the initial slope of the photosynthetic curve (μmol TCO_2 mg chl^{-1} hr^{-1} (μmol photons m^{-2} s^{-1})$^{-1}$).

A multi-dimensional model was fit to determine the combined effects of irradiance and TCO_2 on photosynthetic rate using the function:

$$P = P_{max} \tanh\left(\frac{\alpha I}{P_{max}}\right) + R_d + \beta[TCO_2] \quad (2)$$

where TCO_2 is the initial concentration of DIC (μmol TCO_2 kg^{-1}) for each pCO_2 treatment, and β is the slope corresponding to the observed linear response of photosynthetic rate to the measured TCO_2 concentration. A linear response of photosynthetic rate to TCO_2 concentration was a more accurate predictor than a non-linear function given the range of our experimental TCO_2 concentrations. The estimated maximum photosynthetic rate (P_{max}) and photosynthetic efficiency (α) from the model output was used to calculate the saturation irradiance:

$$I_k = \frac{P_{max}}{\alpha} \quad (3)$$

where I_k is the saturation irradiance and P_{max} and α the outputs from the two-parameter model (eq. 2). P_{max} values across all treatments were then plotted as a function of initial TCO_2 concentration and statistically analyzed using an ANCOVA to determine any significant differences in species' response. In addition, the constructed two-parameter non-linear model (equation 2) was used to predict the hourly photosynthetic potential of each species in Padilla Bay by inputting the *in situ* irradiance data from the field and the initial TCO_2 concentrations from the experiments. The predicted photosynthetic rate (μmol TCO_2 mg chl^{-1} hr^{-1}) from the model output was then used to associate the change in TCO_2 to the potential change in pH and Ω_{ar} over a diurnal light period.

Table 1. Initial conditions for both *Z. marina* and *Z. japonica* experiments. Measured mean values and standard deviation of TA, TCO_2, temperature, salinity, and calculated values pH (total), and aragonite saturation state (Ω_{ar}).

Experiment	pCO_2 treatment	TCO_2 (µmol kg-1)	TA (µmol kg-1)	pCO_2 (µatm)	pH (total)	Ω_{ar}	Temp. °C	Sal. $^0/_{00}$
Z. marina	140	1779 ± 2.7	2157 ± 15	140 ± 4.4	8.40 ± 0.01	4.0 ± 0.0	14.2 ± 0.8	32
	250	1873 ± 4.5	2157 ± 6.3	225 ± 4.0	8.24 ± 0.01	3.0 ± 0.1	14.4 ± 0.6	32
	400	1972 ± 1.8	2141 ± 7.4	421 ± 6.6	8.01 ± 0.01	1.9 ± 0.0	14.0 ± 0.2	32
	650	2083 ± 2.1	2197 ± 5.5	652 ± 18	7.85 ± 0.01	1.4 ± 0.0	14.4 ± 0.3	32
	900	2106 ± 1.5	2180 ± 1.2	863 ± 15	7.73 ± 0.01	1.1 ± 0.0	14.1 ± 0.3	32
Z. japonica	140	1770 ± 6.1	2147 ± 6.2	138 ± 1.8	8.41 ± 0.00	3.9 ± 0.1	14.0 ± 0.5	32
	250	1868 ± 1.1	2147 ± 2.1	214 ± 4.8	8.26 ± 0.01	3.0 ± 0.0	13.6 ± 0.4	31
	400	1956 ± 1.5	2127 ± 1.9	393 ± 8.4	8.03 ± 0.01	1.9 ± 0.0	13.6 ± 0.4	31
	650	2018 ± 0.8	2113 ± 6.2	684 ± 9.6	7.81 ± 0.01	1.2 ± 0.0	13.5 ± 0.3	32
	900	2051 ± 1.7	2103 ± 3.2	918 ± 15	7.70 ± 0.01	0.9 ± 0.1	13.2 ± 0.1	30.5

Results

Incubation conditions. Experimental conditions for the leaf segment incubations were similar between experiments (Table 1). Temperature averaged 13.2 ± 0.4°C, increasing slightly over the duration of the *Z. marina* experiment, but remained stable at 13.4 ± 0.1°C for the *Z. japonica* experiment. Any possible confounding effect of temperature on photosynthetic rate was likely captured within the treatment variance due to the ordinal manner in which replicate vials were terminated. The pCO_2 of the treatments did not match that of the equilibrating gas, which ranged from 100 – 1200 µatm (see Table 1 for actual pCO_2), however, the treatment values did produce a large range in TCO_2 and were similar across both experiments. Actual pCO_2 values will be referred to henceforth as treatment values and for all calculations. The high pCO_2 treatment had the greatest difference between experiments, resulting in a pCO_2 that was 55 µatm higher for the *Z. japonica* experiment than for the *Z. marina* experiment (Table 1). It should be noted that sample size by treatment varied from 20 – 17 (Table 2) due to either loss of a sample or dissolved inorganic carbon analyzer malfunction.

P vs. E curves. The net photosynthetic rates for *Z. marina* and *Z. japonica* were characteristic of autotrophs (Fig. 2a-e), increasing photosynthetic rate with irradiance, and reaching an asymptote once light was saturating. The hyperbolic tangent function described by Jasspy and Platt (1976) fit the general trend of the P vs. E curves (eq. 1), but the photosynthetic parameters P_{max} and α predicted from the model were not well constrained due to the high variance within pCO_2 treatments (Table 2). The robustness of the overall model fit for all treatments was low as indicated by a high RMSE (Fig. 2a-e, Table 2). A conspicuous trend of increasing photosynthetic rate by *Z. japonica* with increasing TCO_2 was observable. The

estimated P_{max} for *Z. japonica* was greater than *Z. marina* when normalized to chlorophyll, with a difference that increased from 0 – 62 μmol TCO_2 mg chl^{-1} hr^{-1} as target treatments increased from 140 – 650 μatm (Fig. 2a-e). When normalized to dry-weight, however, there was no observable difference in P_{max} or α between species, and variance was considerably larger than when normalized to chlorophyll (Appendix A). While we acknowledge that biomass-normalized results may suggest different conclusions than data normalized to chlorophyll, we choose to focus our discussion on the data with chlorophyll standardization because of the microscale changes that are present in photosynthetic pigment content along a leaf (Enríquez et al. 2002).

Respiration rates determined from the darkened and opaque vials were not statistically different across pCO_2 treatments (Appendix B). There was high variance and net photosynthesis occurring within the darkened treatment replicates for both species (Fig. 2a-e, Appendix C). We were, therefore, not able to quantitatively predict respiration rates from our model fit.

Table 2. Predicted photosynthetic parameters from hyperbolic tangent model (Eq. 1) where P_{max} is the maximum photosynthetic rate, α is the photosynthetic efficiency, and R_d is the respiration rate normalized to mg chl. Errors are 95% CI for individual parameters, and the root mean square error (RMSE) of the model fit.

Species	pCO_2 treatment	P_{max}	α	R_d	n	RMSE
Z. marina	140	137 ± 59	0.651 ± 0.60	11.9 ± 43	20	48.3
	250	142 ± 103	0.324 ± 0.48	1.42 ± 32	18	34.2
	400	115 ± 39	2.18 ± 1.8	−12.0 ± 34	20	32.1
	650	94.8 ± 37	0.469 ± 0.45	4.53 ± 27	20	30.8
	900	138 ± 60	2.78 ± 3.4	−3.41 ± 52	20	51.3
Z. japonica	140	283 ± 88	3.01 ± 2.2	−50.5 ± 73	20	74.2
	250	406 ± 181	10.3 ± 11	−96.2 ± 153	17	143
	400	368 ± 175	4.06 ± 7.6	60.5 ± 141	18	152
	650	448 ± 254	4.41 ± 7.3	69.8 ± 210	19	216
	900	337 ± 151	4.91 ± 5.2	21.2 ± 130	19	123

Units: P_{max} and R_d = μmol TCO_2 mg chl^{-1} hr^{-1}; α = μmol TCO_2 mg chl^{-1} hr^{-1} (μmol photons m^{-2} s^{-1})$^{-1}$.

a.

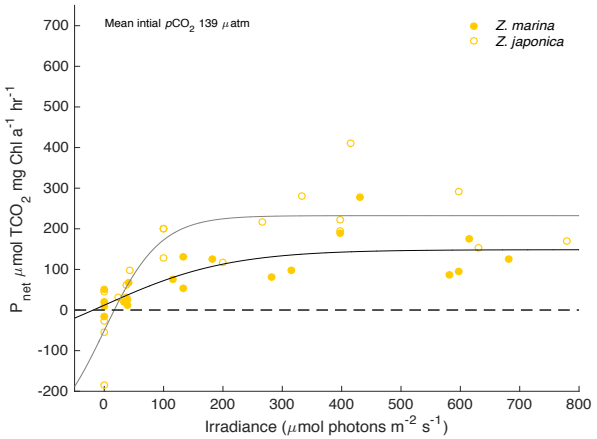

b.

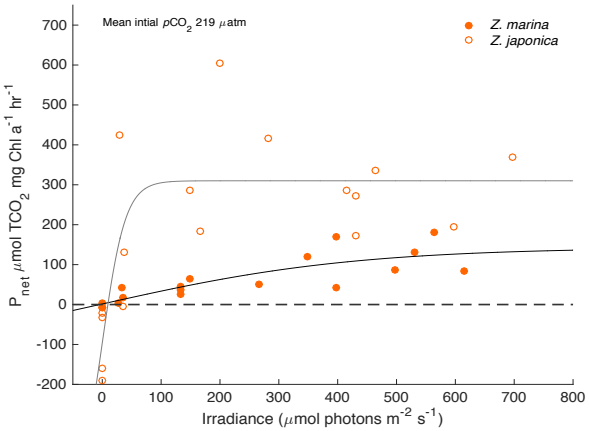

c.

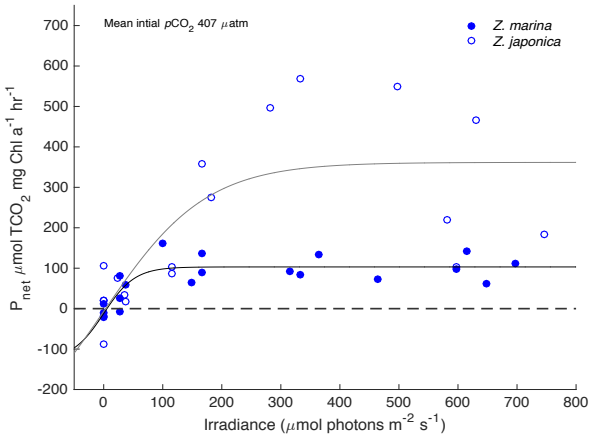

d.

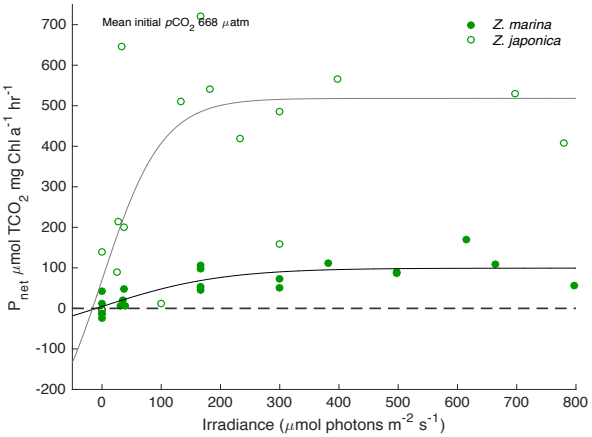

e.

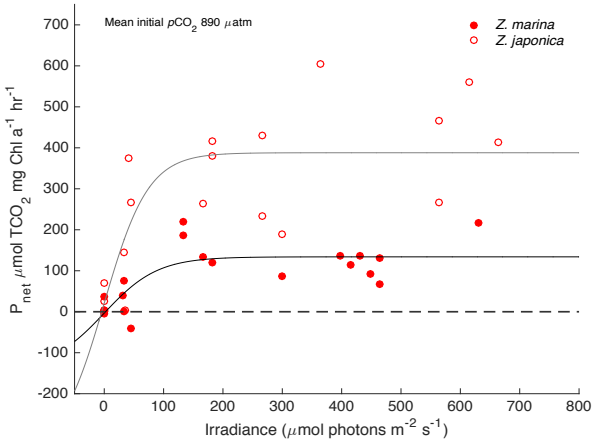

Figure 2. *P* vs. *E* curves at each mean initial pCO_2 (a) 139 µatm, (b) 219 µatm, (c) 407 µatm, (d) 668 µatm, and (e) 890 µatm (i.e., initial pCO_2 for both experiments were averaged to obtain mean initial pCO_2). Open circles are *Z. japonica* and closed circles are *Z. marina* photosynthetic rates (µmol TCO_2 mg chl^{-1} hr^{-1}). Dashed black line is irradiance compensation. Negative values are respiration.

Two-parameter photosynthesis model. Net photosynthetic rates were collated across treatments for both species and fit to the combined hyperbolic tangent and linear functions describing the observed relationship of photosynthesis to irradiance and TCO_2, respectively (Fig. 3, Eq. 2). Using the entire data set and incorporating irradiance and TCO_2 resulted in a more robust prediction of the photosynthetic parameters, and a clear delineation of the species' differential response (Fig. 4). *Z. japonica* displayed a P_{max} of 360 ± 74 μmol TCO_2 mg chl^{-1} hr^{-1} and an α of 3.62 ± 2.1 μmol TCO_2 mg chl^{-1} hr^{-1} (μmol photons m^{-2} s^{-1})$^{-1}$ where the error is the 95% CI (Table 3). Both P_{max} and α were significantly higher for *Z. japonica* than for *Z. marina*, which had a P_{max} of 113 ± 21 μmol TCO_2 mg chl^{-1} hr^{-1} and an α of 0.840 ± 0.42 μmol TCO_2 mg chl^{-1} hr^{-1} (μmol photons m^{-2} s^{-1})$^{-1}$ where the error is the 95% CI (Table 3, Fig. 4). P_{max} for *Z. japonica* was 3x greater than *Z. marina* P_{max}, and α was 4x greater, indicating an overall higher maximum photosynthetic rate and efficiency for *Z. japonica* on a per chlorophyll basis. In addition, *Z. japonica* displayed a lower I_k at 99 (propagated SE = 31) μmol photons m^{-2} s^{-1}, which was ~ 75% of *Z. marina*'s I_k of 131 (propagated SE = 35) μmol photons m^{-2} s^{-1}. Error for both I_k values is the propagated standard error from model predicted P_{max} and α (Eq. 3).

TCO_2 concentration and the TCO_2 species interaction were both significant predictors of P_{max} (Table 4). The ordinal interaction between TCO_2 and species indicates a differential species' response of P_{max} to increasing TCO_2. The mean P_{max} of *Z. japonica* increased linearly with TCO_2 across all treatments, whereas *Z. marina* P_{max} appeared constant with increasing TCO_2 (Fig. 5). Since there was an interaction effect between the main effects TCO_2 and species, and no observable response of *Z. marina* to increasing TCO_2, further analysis was warranted. A one-way ANOVA examining the effect of initial TCO_2 on P_{max} determined there was a significant difference in mean P_{max} between initial TCO_2 concentrations for *Z. marina*: $F_{4,53} = 3.01$, p =

0.0258). Given the high degree of variability and low *F*-ratio, however, *Z. marina*'s P_{max} response to TCO_2 remains unclear based on our findings. *Z. japonica*'s P_{max} increased by ~150 μmol TCO_2 mg chl^{-1} hr^{-1} over the range of initial TCO_2 concentrations (Fig. 5). The increase in *Z. japonica* P_{max} to increasing TCO_2 resulted in a broadening separation of the maximum photosynthetic rate potential between the two species at higher TCO_2 conditions (Fig. 5*)*.

a.

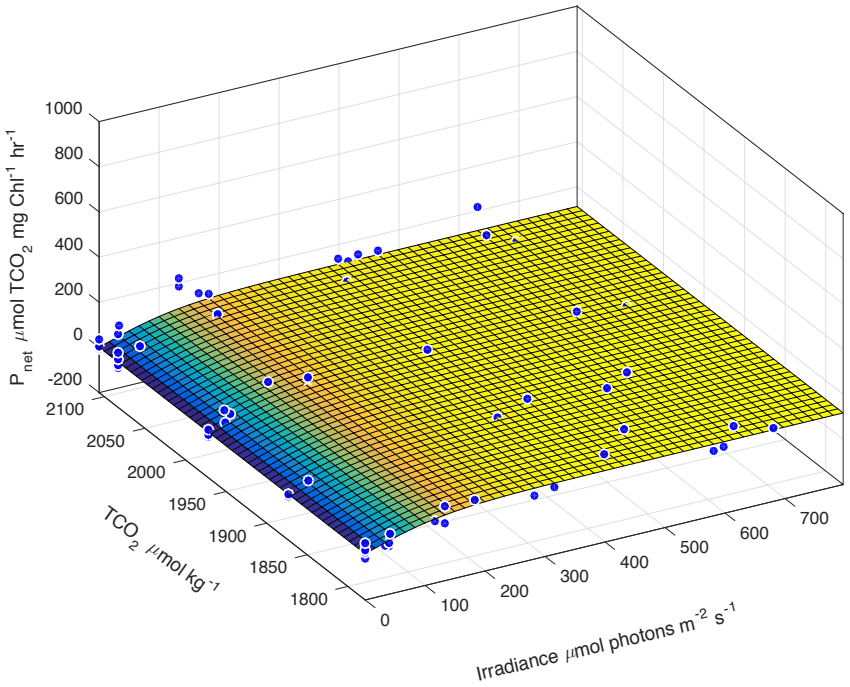

b.

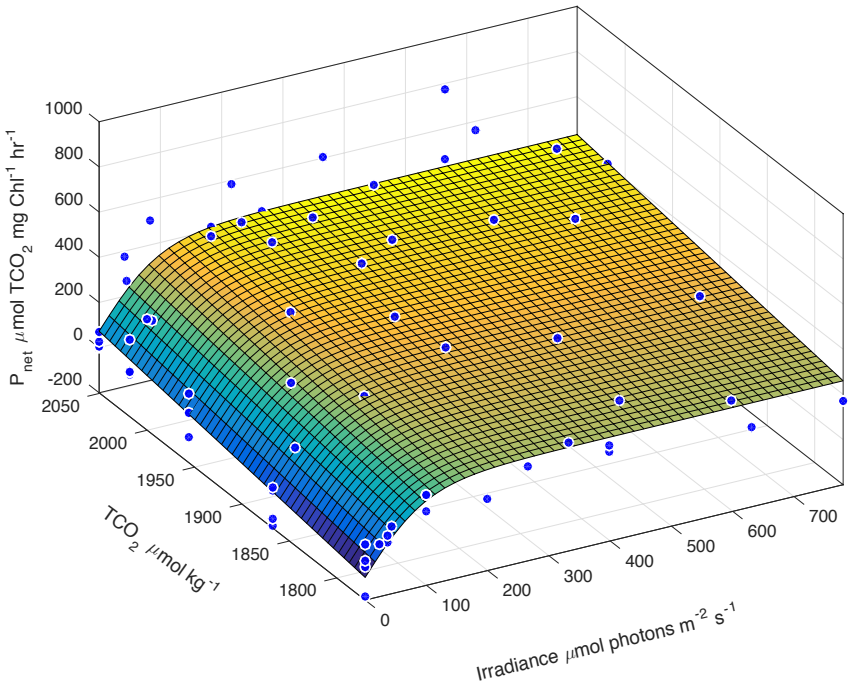

Figure 3. Net photosynthetic rate across all pCO_2 treatments for (a) *Z. marina* and (b) *Z. japonica* as a function of irradiance and TCO_2. TCO_2 values are initial concentrations corresponding to each pCO_2 treatment (Table 1).

Table 3. Predicted photosynthetic parameters from non-linear regression model (Eq. 2) with irradiance and TCO_2 as independent variables. β is the slope of linear relationship between photosynthetic rate and initial TCO_2 concentrations. Total sample size for *Z. marina* and *Z. japonica*: n =98 and n = 93, respectively.

Species	Parameter	Estimate	SE	95% CI	tstat	p-value
Z. marina	P_{max}	113	10.7	21.3	20	48.3
	α	0.840	0.211	0.420	18	34.2
	R_d	24.7	69.6	138	20	32.1
	β	−0.011	0.035	0.069	−0.327	0.745
Z. *japonica*	P_{max}	360	37.2	73.9	9.68	< 0.001
	α	3.62	1.06	2.12	3.40	0.001
	R_d	−1185	286	568	−4.15	< 0.001
	β	0.613	0.147	0.292	4.18	< 0.001

Units: P_{max} and R_d = μmol TCO_2 mg chl^{-1} hr^{-1}; α = μmol TCO_2 mg chl^{-1} hr^{-1} (μmol photons m^{-2} s^{-1})$^{-1}$.

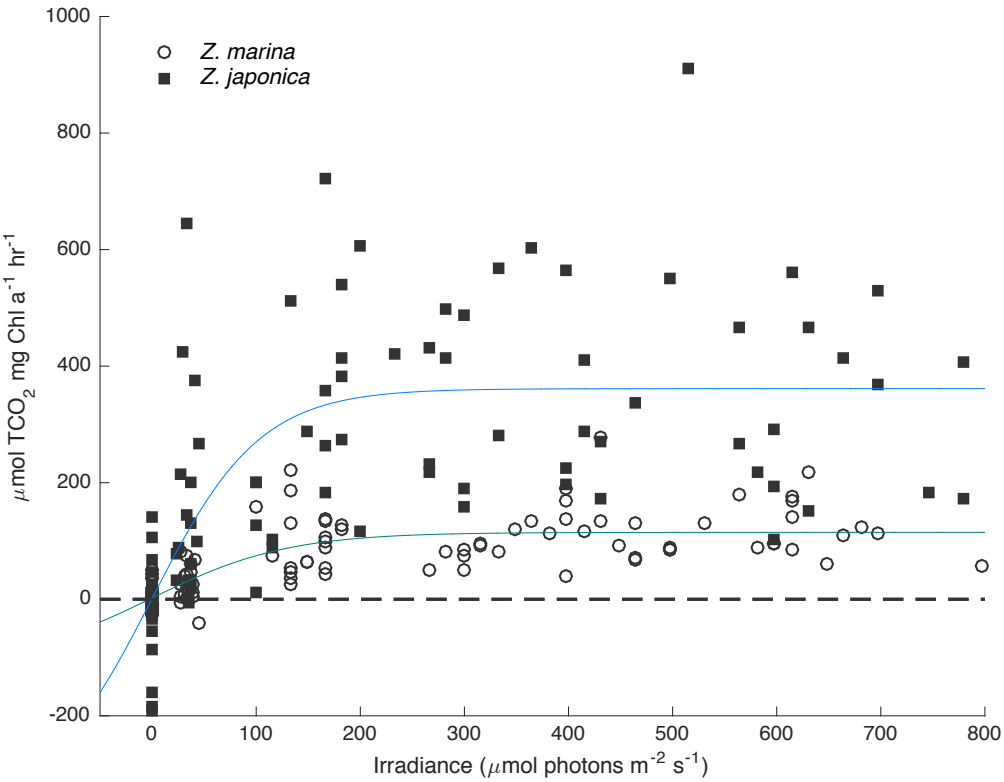

Figure 4. P vs. E curves for *Z. marina* (open circles) and *Z. japonica* (closed squares) for all net photosynthetic rates collated from every pCO_2 treatment.

Table 4. ANOVA table from ANCOVA analysis examining P_{max} values with main effects TCO_2 and species.

Source	d.f.	Sum Sq	F-stat.	p-value
Species	1	1.60E+06	109	< 0.001
TCO_2	1	1.27E+05	8.67	0.004
Species*TCO_2	1	1.96E+05	13.4	< 0.001
Error	109	1.60E+06	•	•

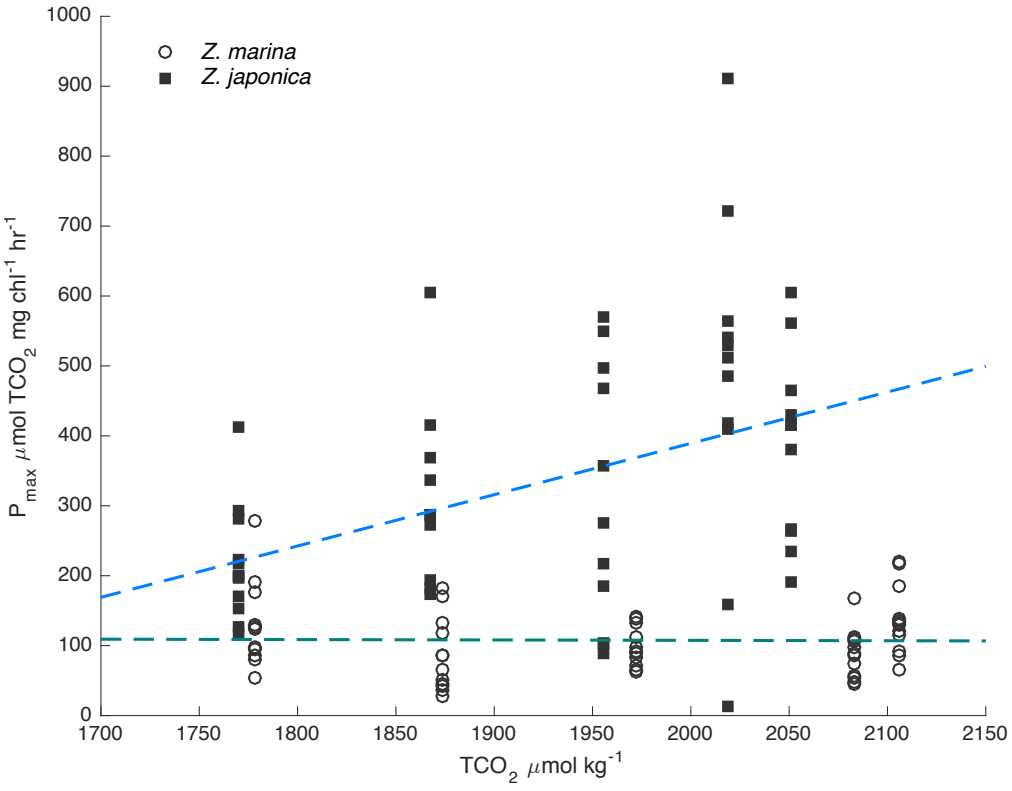

Figure 5. Maximum photosynthetic rate (P_{max}) of *Z. marina* (open circles) and *Z. japonica* (closed squares) as a function of initial TCO_2 concentration. Initial TCO_2 concentrations correspond to each pCO_2 treatment (Table 1). P_{max} values are photosynthetic rates above I_k, which was predicted from the model fit for *Z. marina* (131 µmol photons m^{-2} s^{-1}) and *Z. japonica* (99 µmol photons m^{-2} s^{-1}).

Model predictions and field irradiance. Irradiance data from the field, and average TCO_2 concentrations from both experiments (1972 μmol kg^{-1} for *Z. marina* and 1956 μmol kg^{-1} for *Z. japonica*) corresponding to the median 400 pCO_2 treatment were input into the two-parameter photosynthesis model to estimate the hourly change in photosynthetic rate for both species in Padilla Bay. The predicted net photosynthesis for *Z. japonica* reached a maximum of 379 μmol TCO_2 mg chl^{-1} hr^{-1} and 115 μmol TCO_2 mg chl^{-1} hr^{-1} for *Z. marina* for ~6 hours; this indicates that saturating irradiance for both species likely occurs from ~12:00 until ~18:00 during mid to late summer (Fig. 6). The upper and lower bounds are the predicted photosynthetic rate for *Z. japonica* if TCO_2 concentrations were 2051 μmol kg-1 and 1771 μmol kg^{-1}, which correspond to the high (pCO_2 ~900) and low (pCO_2 ~140) treatments, respectively (Fig. 6).

The predicted photosynthetic rate (μmol TCO_2 mg chl^{-1} hr^{-1}) over a diurnal period was used to estimate the change in TCO_2 from a starting point of 1964 μmol kg^{-1}. These values were then used to determine the associated change in pH and Ω_{ar} mg chl^{-1} hr^{-1} assuming a constant TA (Fig. 7). A combined average TA of the 400 pCO_2 treatment for both experiments was used for all calculations. *Z. japonica* induced a maximum change in pH of 0.65 units mg chl^{-1} hr^{-1} at a P_{max} of 379 μmol TCO_2 mg chl^{-1} hr^{-1}. The induced change in pH by *Z. japonica* was ~0.4 units higher than the 0.25 pH unit change associated with *Z. marina*'s P_{max} of 115 μmol TCO_2 mg chl^{-1} hr^{-1} (Fig. 7). The Ω_{ar} change associated with the projected maximum photosynthetic rate for both species resulted in a change of 3.8 and 1.1 mg chl^{-1} hr^{-1} for *Z. japonica* and *Z. marina*, respectively. It should be noted that the change in pH was determined from the change in TCO_2 from a single seagrass segment in a 20 ml vial, and estimations beyond this scale are likely erroneous. We, therefore, present the change in pH and Ω_{ar} as the maximum potential possible

based on our findings, where extrapolation is constrained within direct proximity to a portion of a seagrass leaf.

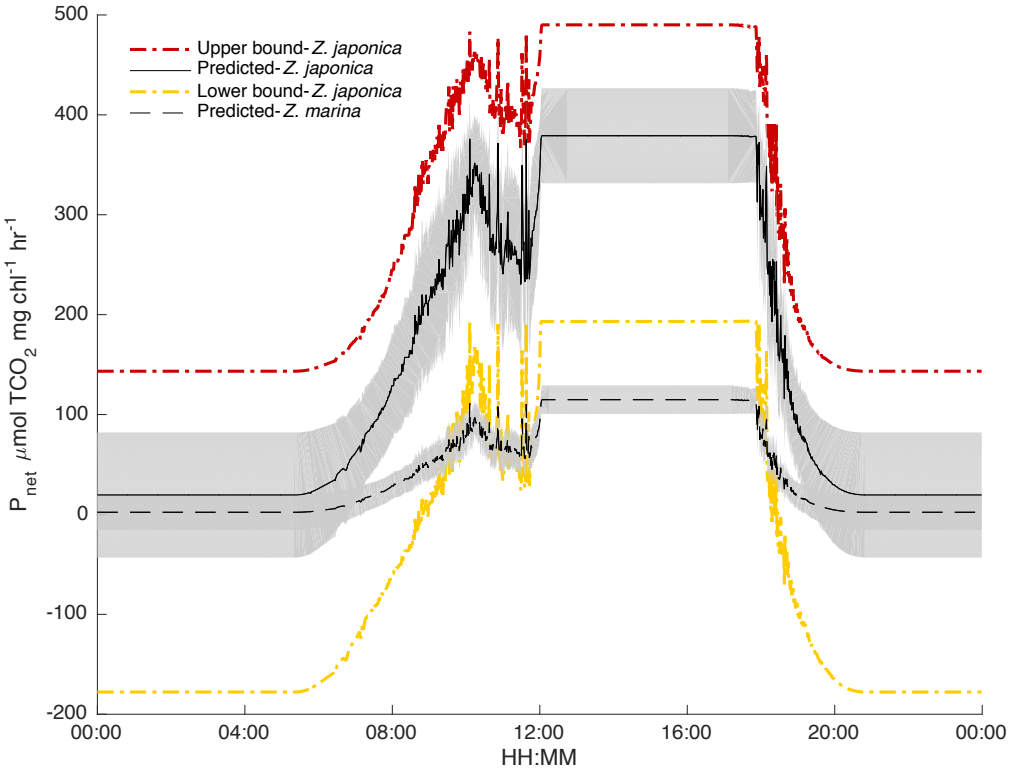

Figure 6. Predicted mean net photosynthetic rate for *Z. japonica* (-) and *Z. marina* (--) under ambient irradiance at mean initial TCO_2 concentration of 1964 µmol kg^{-1}. Shaded region is the 95% CI. Upper (red) and lower (yellow) bounds are the predicted net photosynthetic rate of *Z. japonica* at initial TCO_2 concentrations of 2051 and 1770 µmol kg^{-1}, respectively.

a.

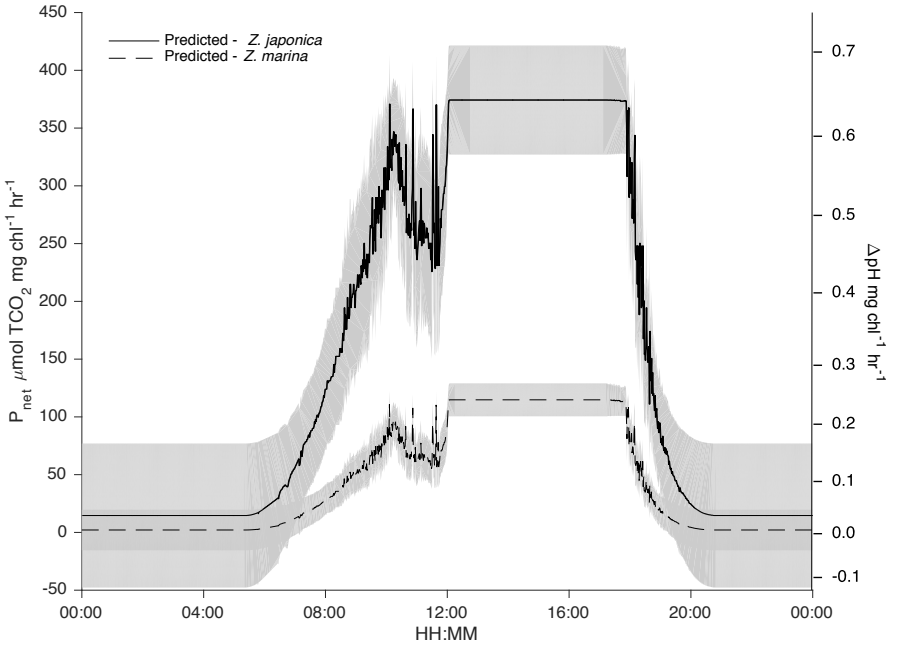

b.

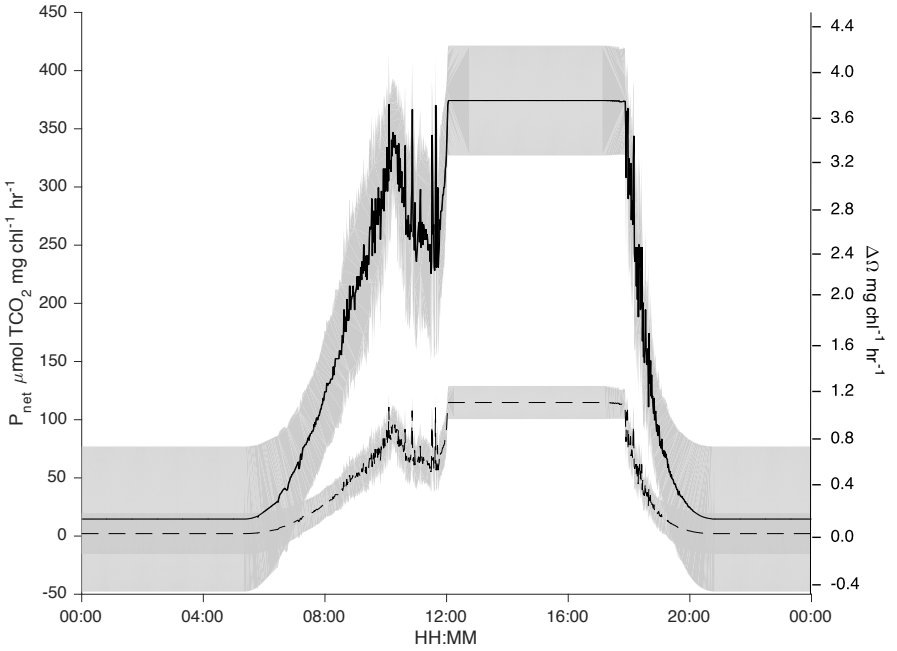

Figure 7. Change in pH_{total} (a) and Ω_{ar} (b) at the predicted mean net photosynthetic rate for *Z. japonica* (-) and *Z. marina* (--) under ambient irradiance. Shaded regions are the 95% CI for photosynthetic rate.

Discussion

Species-specific photosynthetic rate and TCO_2 uptake are critical components that determine the capacity of seagrasses to remove dissolved CO_2 and, thus, the potential of seagrass beds as OA refugia. This study examined the photosynthetic potential of co-occurring *Z. marina* and *Z. japonica* seagrasses to a range of TCO_2 concentrations. Our results indicate that *Z. japonica* photosynthesis has a robust response to moderate increases in TCO_2, whereas *Z. marina* photosynthesis displays a minor or null response to the TCO_2 concentrations tested (~1770 – 2100 μmol kg^{-1}). These findings help elucidate how TCO_2 dependent instantaneous photosynthetic rates of *Z. marina* and *Z. japonica* will affect the carbonate system, and what implications exist for potential OA mitigation on short timescales. That is, if seagrasses are to mitigate the effects of acidification on vulnerable organisms, the timing of TCO_2 uptake and shift in favorable carbonate chemistry must be congruent with the organismal life-stages that are most sensitive to acidification. For example, recent studies have shown that the initial shell formation of *Crassostrea gigas* occurs in a matter of hours, and unfavorable carbon chemistry affects the development and growth of some bivalves and gastropods during the first 48 hours post-fertilization (Onitsuka et al. 2014, Waldbusser et al. 2015b). Instantaneous photosynthetic rates occurring on the hourly timescale, therefore, can correspond directly to the time period of shell formation for some bivalves, and have the potential to dampen the magnitude and exposure duration to acidification.

Instantaneous photosynthesis. The instantaneous photosynthetic rates measured indicate that non-native populations of *Z. japonica* in Padilla Bay have a maximum net photosynthetic rate and efficiency that is ~3 and 4.5-fold higher, respectively, than *Z. marina* occurring in the

same intertidal spatial zone when considered on a per chlorophyll basis. We did not observe inter-species differences when standardized to biomass (App. Table 2). Whereas the exact mechanism responsible for the discontinuity between standardization methods is not clear, standardizing to chlorophyll is more appropriate given the strong gradient in chlorophyll along a leaf and among shoots, which may correspond to changes in surface area and, therefore, pigment concentration (Zimmerman et al. 1997, Enríquez et al. 2002, Larkum et al. 2006 and references therein). Given that changes in thickness of the tissue can affect chlorophyll to biomass ratio (Enríquez et al. 1994), photosynthetic rate standardized to biomass may account for spatial variation in chlorophyll and how light is absorbed.

Similarly, a previous study comparing PNW populations of *Z. marina* and *Z. japonica* also found that *Z. japonica* has a maximum photosynthetic rate that is ~3-fold higher than *Z. marina*, when exposed to the same light conditions (Shafer and Kaldy 2014). The chlorophyll standardized rates reported in that study and in Shafer et al. (2011), however, were considerably lower than what we report (Fig. 2a-e). Differences in chlorophyll extraction methods, or inefficient extraction may have resulted in the higher photosynthetic rates found in our study. Additional factors such as intertidal location, canopy density, time of year, acclimatization to epiphytic growth, and age can also affect pigment concentration and photoacclimation amongst shoots and along leaves (Dennison and Alberte 1986, Major and Dunton 2002, Enríquez et al. 2002, Duarko and Kunzelman 2002, Drake et al. 2003, Cummings and Zimmerman 2003, Larkum 2006 and references therein), which may further explain the dissimilarity in rates. Local acclimatization to *in situ* temperature and salinity can also impact photosynthetic rates via osmotic stress and changes in the photosynthesis-respiration ratio (Kenneth and Short 2006 and references therein). In addition, our study examined photosynthetic rates by measuring the

change in TCO_2, which to our knowledge, has not been done before in the lab and rarely done in the field despite the robustness of the method (Silva et al. 2009). The photosynthetic quotient (O_2/CO_2), while assumed to be unity or close to in many studies, is based on community metabolism in seagrass beds or meadows (Oviatt et al. 1986, Leuschner and Rees 1993, Martin et al. 1995, Mateo et al. 2001); therefore, measuring TCO_2 rather than O_2 may result in photosynthetic rates that are dissimilar if the photosynthetic quotient is not close to unity under these conditions. That is, based on the higher photosynthetic rates found in this study, the change in CO_2 per O_2 would have to be much lower in seagrass communities than what was measured in our vials. Additionally, recycling and movement of gases within the lacunal system are not well understood (Mateo et al. 2001), further convoluting the comparison of instantaneous O_2 production and CO_2 uptake. Measurement of TCO_2 for our study, however, is appropriate given that carbon drawdown specifically, rather than photosynthetic rates, drives OA mitigation potential of seagrasses.

Effects of TCO_2. Increases in TCO_2 enhanced the maximum photosynthetic rate for *Z. japonica*, while *Z. marina*'s response was inconclusive (Fig. 5). Even though statistical analysis found a significant difference between mean P_{max} values across initial TCO_2 concentrations for *Z. marina*, the level of significance was minor ($F_{4,53} = 3.01$, $p = 0.0258$). Across treatments, there was no observable increase in *Z. marina* P_{max} and, therefore, no apparent trend of increasing P_{max} with increasing TCO_2. An effect size of 19% was determined from the one-way ANOVA analysis (Appendix D), meaning that only 19% of P_{max} variance was attributable to initial TCO_2 concentration. The lack of enhanced photosynthesis by *Z. marina* in response to increasing TCO_2 is clearly contradictory to what has been previously reported for instantaneous photosynthetic

rates (Beer and Koch 1996, Thom 1996, Zimmerman et al. 1997); however, the manipulated TCO_2 concentrations in those studies were, at minimum, 25% higher than our highest TCO_2 concentration. It is likely that the range of TCO_2 concentrations used for this study was not large enough to produce a response of increased P_{max} for *Z. marina* that could be detected given the high variability within our treatments. Zimmerman et al. (1997) showed that *Z. marina* increased its P_{max} 225% with an exposure to TCO_2 77% higher than ambient (from 2074 to 3673 μmol kg^{-1}). Over this range of TCO_2, a linear relationship exists between P_{max} and TCO_2 (Beer and Koch 1996). Using a linear equation derived from Zimmerman et al. (1997) and our mean P_{max} values at the lowest and highest TCO_2 concentrations, an 18% increase in TCO_2 would induce a 55% increase in *Z. marina* P_{max}. Given that the coefficient of variation (CV) ranged from 30 to 60% over all initial TCO_2 concentrations, any response to TCO_2 by *Z. marina* was likely obscured by the variance. Interestingly, however, a robust response was observed for *Z. japonica*, which increased its mean P_{max} 55% over the 18% increase in TCO_2, despite a CV identical to *Z. marina* (30 – 60%). Physiological and methodological factors contributing to the large variance within treatments may be a result of shoot to shoot variability of the photosynthetic apparatus, and the propagation of a diffusive boundary layer due to incremental stirring, which would increase the variability of the relative TCO_2 conditions experienced by the leaf segment compared to the entire vial.

The range of pCO_2 values and corresponding TCO_2 concentrations (Table 1) used for this study are representative of present day conditions in Padilla Bay, which exhibit large diurnal fluctuations in carbonate chemistry (Love et al. 2016). Based on our findings, *Z. japonica* will have a substantially greater response to TCO_2 fluctuation than will *Z. marina* in Padilla Bay. The differential response of P_{max} to TCO_2 between species may be due to the mechanism by which

HCO_3^- is utilized for photosynthesis. Evidence suggests that seagrass occurring in the intertidal, such as the *Z. marina* samples in our study, are adapted to more efficiently utilize HCO_3^- than seagrass found at depth (Schwarz et al. 2000). *Z. marina* has been shown to take up HCO_3^- as an inorganic carbon source via external carbonic anhydrase (CA) secretion, and is saturated with respect to HCO_3^- at pH from 7.5 – 8.5 (Beer and Rehnberg 1996, Invers et al. 2001, Koch et al. 2013), which, corresponds to the range of pH values in our study (Table 1). Since HCO_3^- appears saturating at present day and future TCO_2 levels for *Z. marina*, and any enhanced effect of CO_2 will be greater when pH is less than ~7.5, our results suggest that *Z. japonica* either has a lower pH threshold at which CO_2 concentrations are high enough to elicit enhanced photosynthetic rates, or that HCO_3^- concentrations are not saturating over the range of TCO_2 concentrations used in this study.

Given that there are significant variations in the ability to utilize HCO_3^-, and that some species have a capacity to more efficiently utilize HCO_3^- depending on the mechanisms exploited (Invers et al. 2002, Koch et al. 2013, Campbell and Fourqurean 2016) we, therefore, suggest that *Z. japonica* is less efficient than *Z. marina* in HCO_3^- uptake. While we did not specifically measure the ability or mechanism of HCO_3^- uptake in either species, there appears to be a higher threshold at which HCO_3^- becomes saturating for *Z. japonica*, as evident by the shape of the response of increased P_{max} to HCO_3^- (Fig. 8a). The linear response of increased P_{max} to HCO_3^- is analogous to the response observed in figure 5 to TCO_2. This suggests that the dominant driver of enhanced photosynthetic rate over the range of TCO_2 tested is likely a response to HCO_3^- and not CO_2, which produces a different P_{max} response curve (Fig. 8b). Evidence supports that *Z. marina* has established mechanisms to efficiently use HCO_3^- (Beer and Rehnberg 1997, Invers et al. 2001) when CO_2 concentrations are low; however, the mechanisms of HCO_3^- utilization by *Z.*

japonica remain unknown. If *Z. japonica* is indeed able to increase its maximum photosynthetic rate when HCO_3^- concentrations are higher, than *Z. japonica* may be one of the few seagrass species to respond positively to moderate increases in seawater TCO_2, thus providing an increasingly more beneficial role in OA mitigation over *Z. marina*.

The high energetic cost behind HCO_3^- utilization is due to the active mechanisms by which it occurs: H^+ pumping and CA secretion (Larkum 2006 and references therein, Koch et al. 2013); therefore, an energetic constraint may be a reason as to why HCO_3^- uptake may not be as efficient for *Z. japonica*. Due to its distribution predominately in the high intertidal (Shafer et al. 2014), *Z. japonica* likely has to invest more energy into maintaining osmotic and thermal homeostasis due to the higher extremes of irradiance and salinity that occur throughout its distribution in the intertidal. Previous studies have found that *Z. japonica* invests in high concentrations of UV protective pigments and can tolerate chronic hypo and hyper saline conditions (Kaldy 2006, Shafer et al. 2011). Energy investment into these physiological characteristics which enable tolerance of unfavorable thermal and osmotic pressures likely result in a tradeoff, or lack of investment in other processes, such as active HCO_3^- utilization. This does not, however, contradict the overall greater photosynthetic potential displayed by *Z. japonica* when TCO_2 concentrations are not elevated. Rather, mechanisms other than CO_2 substrate availability may be the reason for higher yields, such as the structure of the photosynthetic package, which determines the reflectance and absorbtance by the photosynthetic pigments (Cummings and Zimmerman 2003, Zimmerman et al. 2006).

The differential response of *Z. marina* and *Z. japonica* to increasing TCO_2 has implications for species' success, performance, and expansion in a high CO_2 world. Based on our findings, it is likely that *Z. japonica* will benefit more from the increasing CO_2 baseline due to its

ability to increase HCO_3^- utilization (Fig. 8a) as well as benefiting from increased CO_2 uptake. The greater response of *Z. japonica* to TCO_2 will lead to an increase in growth rate for above and below ground biomass. The increase in growth, however, does not necessarily translate to an increased competition effect with *Z. marina*. Evidence suggests that *Z. japonica* distribution offshore (i.e., an encroaching presence into *Z.* marina's upper distribution) is limited by temperature, and that the morphological difference between the two species results in a competitive dominance of *Z. marina* over *Z. japonica* due to its broader leaves and canopy height, which shade *Z. japonica* (Harrison 1982b , Kaldy et al 2015). While *Z. japonica* presence offshore is less likely due to thermal tolerance and competition with *Z. marina*, its continued colonization of unvegetated habitat higher in the intertidal may increase if growth is enhanced at higher TCO_2. The expansion into unvegetated habitat could provide additional ecological benefits for species (Shafer et al. 2014), as well as a spatial expanse of seagrass induced modification of carbonate chemistry throughout the intertidal zone.

a.

b.

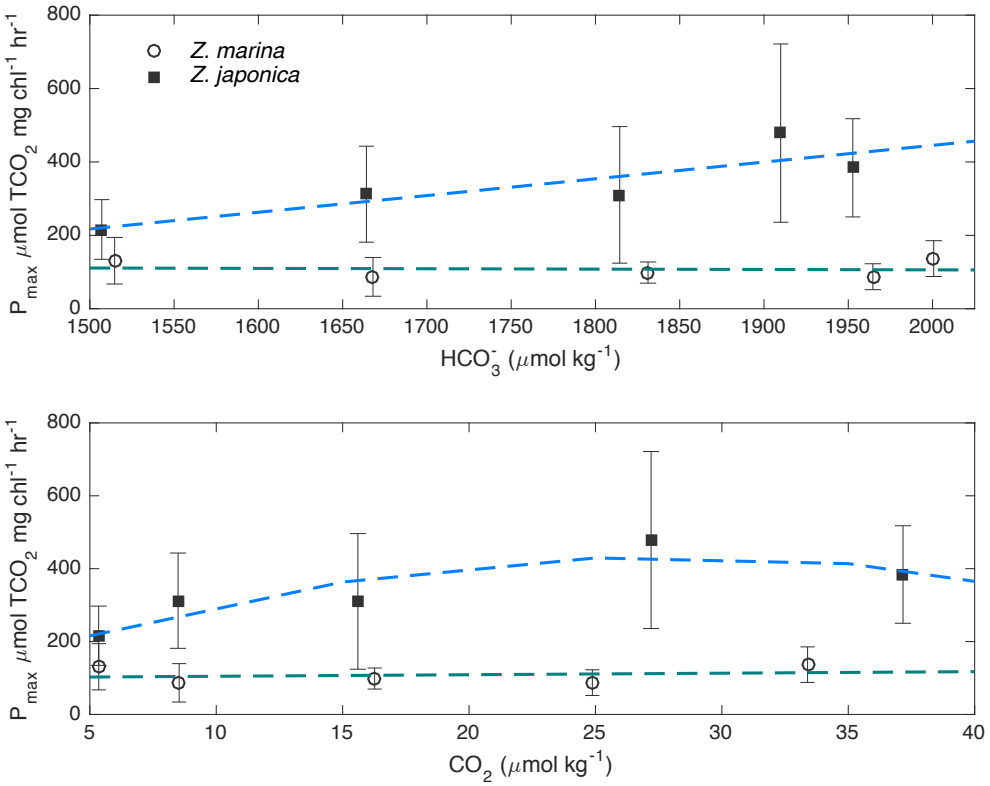

Figure 8. Mean maximum photosynthetic rate (P_{max}) of *Z. marina* (open circles) and *Z. japonica* (closed squares) as a function of HCO_3^- (a) and CO_2 (b). Error bars are SD. Discrete HCO_3^- and CO_2 concentrations are the initial values for each treatment corresponding to pCO_2 and TCO_2 values (Table 1). Teal dashed lines are the linear fit applied to *Z. marina*'s response to HCO_3^- and CO_2. Blue dashed lines are the linear (a) and non-linear (2nd order polynomial) (b) best fit of *Z. japonica*'s P_{max} to HCO_3^- and CO_2.

Predicting OA mitigation potential. Measuring instantaneous photosynthetic rates of *Z. marina* and *Z. japonica* as a change in TCO_2, and assuming alkalinity constant, provides a constraint on the carbonate system; thereby providing a means to predict how the photosynthetic potential of each species will affect the carbonate chemistry of the surrounding water. Light sensor data from the field and initial TCO_2 concentrations were used to parameterize the two-parameter irradiance-TCO_2 model (Fig. 3), and predict how photosynthetic rate changes by the hour for *Z. marina* and *Z. japonica* in Padilla Bay (Fig. 6). Additionally, estimates of the corresponding change in pH and aragonite saturation state were calculated based on the photosynthetic rate of each species (Fig. 7). Importantly, the induced changes on the carbonate system are approximate values and correspond to seawater directly adjacent to a photosynthesizing leaf segment on a microscale level. Nevertheless, this gives better insight as to the potential change in the carbonate system made possible by *Z. marina* and *Z. japonica*. Our results indicate that *Z. japonica* displays a 3-fold higher photosynthetic potential and, therefore, has a stronger affect on the carbonate system on a per chlorophyll basis. Importantly, the estimated changes in pH and Ω_{ar} are only representative at given temperature and salinity (Fig 7).

To integrate our findings into a more applicable context of OA-mitigation, the specific changes induced on the carbonate system by both species' maximum photosynthetic potential were extrapolated to different volumes of water corresponding to various depths over a 1 m^2 patch of seagrass with a biomass of 100 gDW m^{-2}. Biomass estimates from Padilla Bay were approximated from Bulthuis (2013), where gDW m^{-2} ranges from ca. 60 – 200 for both species. Assuming a well-mixed water column, average mg chl gDW^{-1} (C_b) as measured for each species and projected P_{max} values (r) were used to calculate a change in TCO_2 as:

$$\Delta TCO_2 = TCO_{2i}\left(C_b * \left(\frac{b_i}{a}\right) * \left(\frac{1}{d}\right) * f * r\right) \quad (4)$$

where TCO_{2i} is the initial TCO_2 concentration, C_b is mg chl gDW^{-1}, b_i is the gDW m^{-2}, d is depth (m), and f is the unit conversion m^3 1000 L^{-1} (summarized, Table 5). Changes in TCO_2 were then used to determine changes in carbonate chemistry parameters. It is important to note that the chlorophyll to biomass ratio for our experiment was considerably lower than what has been previously reported (Shafer and Kaldy 2014), and inefficiencies in our chlorophyll extraction could overestimate the predicted changes. Despite the differences in our chlorophyll to biomass measurements, the general trend and relative difference between *Z. marina* and *Z. japonica* photosynthesis on carbonate chemistry is clear. Specifically, the change in pH, aragonite saturation state, and the substrate-to-inhibitor ratio ($[HCO_3^-]/[H^+]$, all of which have been shown to affect calcification and acid-base regulation of organisms sensitive to acidification (Pörtner 2008, Kroeker et al. 2013, Waldbussser et al. 2015a, b Thomsen et al. 2015, Fassbender et al. 2016) were approximated (Fig. 9). Theses changes, however, are specific to the timescale of TCO_2 uptake via photosynthesis, and will shift with changes in photosynthetic activity and respiration on an hourly scale. While our findings are based on *Z. marina* and *Z. japonica* populations in the lower intertidal of Padilla Bay, extrapolation of the induced changes on the carbonate system by species-specific photosynthesis may be applicable to other locales with similar physical conditions and ecological structure. Importantly, the distribution of both species needs to be taken into account when determining the total effect each species has on carbonate chemistry. For example, our findings suggest that *Z. japonica* has a stronger affect on carbonate chemistry than *Z. marina*; however, the 3:1 greater hectare coverage of *Z. marina* in Padilla Bay (Table 5) results in a larger-scale affect by Z. *marina* than *Z. japonica*. In addition, our findings could be applied and referenced when determining aquaculture techniques aimed at improving

carbonate chemistry conditions in more controlled environments, which is an initiative of the shellfish industry in Washington state (Blue ribbon panel on ocean acidification 2012).

Table 5. Analytical and predicted parameters mg chl gDW^{-1}, ΔTCO_2, and P_{max} for *Z. marina* and *Z. japonica*. Parameters were used in conjunction with approximated biomass m^{-2} to calculate changes in the carbonate system (Fig. 9). *Reported from Padilla Bay (PB) in Bulthuis (2013).

Species	Mean initial TCO_2	Mean chl:biomass ratio	Predicted P_{max}	Est. biomass* ($gDW\ m^{-2}$)	Coverage $species^{-1}$ in PB* (ha)
Z. marina	1964	1.88 ± 0.89	115	100	3046
Z. japonica	1770	0.67 ± 0.33	193	100	836
	1964	0.67 ± 0.33	379	100	•
	2051	0.67 ± 0.33	490	100	•

Units: TCO_2 = umol kg^{-1}; P_{max} = µmol TCO_2 mg chl^{-1} hr^{-1}; chl:biomass = mg chl gDW^{-1}.

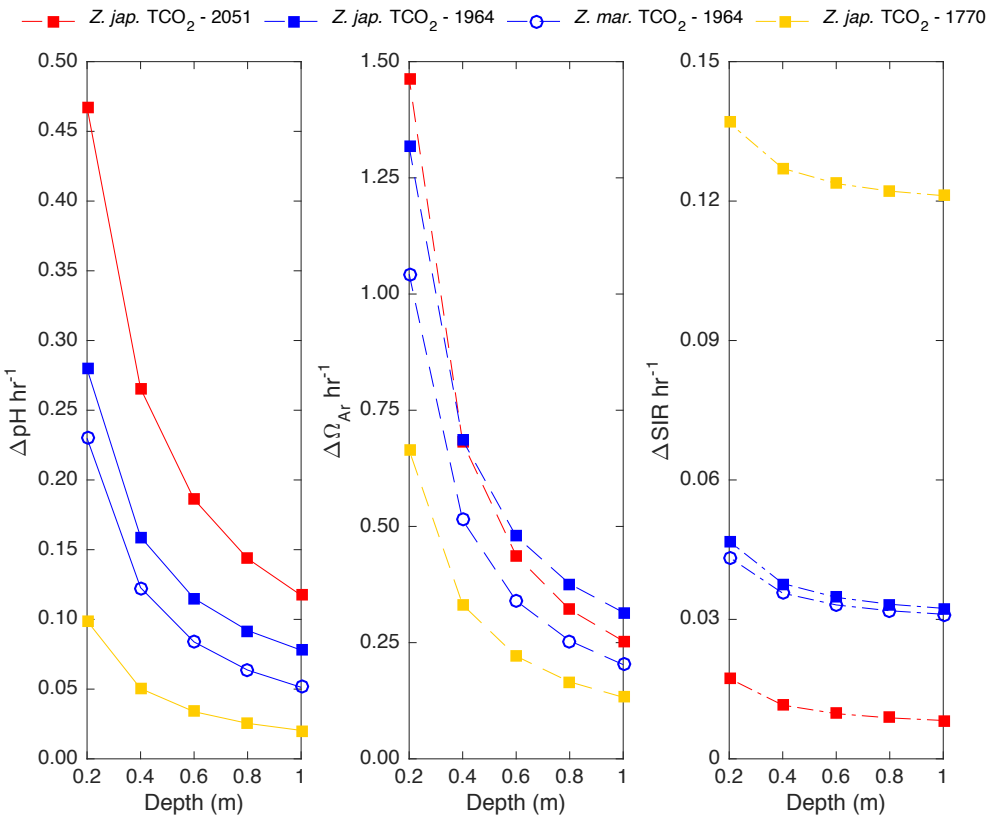

Figure 9. Blue lines are the predicted change in pH, aragonite saturation state, and substrate-to-inhibitor (mol µmol^{-1}) ratio based on the predicted P_{max} (µmol TCO_2 mg chl^{-1} hr^{-1}) of *Z. marina* (open circles) and *Z. japonica* (closed squares) with an initial TCO_2 concentration of 1964 µmol kg^{-1}. Red and yellow lines are the upper and lower bound of the predicted change in pH, aragonite saturation state, and substrate–to-inhibitor ratio of the high and low pCO_2 treatment of *Z. japonica* at initial TCO_2 concentrations of 2051 and 1770 µmol kg^{-1}, respectively. Predicted change is over a 1 m^2 area and given depth assuming a biomass of 100 gDW m^{-2} (Table 5, Eq. 4). Initial TCO_2 concentrations correspond to pCO_2 treatments at specific experimental conditions of TA (TA was averaged for 400 pCO_2 treatment), temperature, and salinity (Table 1).

Dynamics of seagrass beds. Recent studies have highlighted the extreme spatial and temporal variability that exists when attempting to determine potential mitigating effects macrophytes may have on unfavorable carbonate chemistry (Hendriks et al. 2014, 2015, Krause-Jensen et al. 2015, Challener et al. 2016). In addition to seagrass productivity and respiration, heterotrophic respiration, tidal exchange, and riverine input further modify carbonate chemistry on various spatial and temporal scales. Because organisms vulnerable to OA are more sensitive at particular life-stages, the temporal variability of carbonate chemistry becomes critical in determining organismal resilience to OA (Kurihara 2008, Hettinger et al. 2012, Barton et al. 2012, Waldbusser et al. 2015b). Importantly, the spatial heterogeneity of carbonate chemistry within seagrass beds is equally important. Variations in chlorophyll content along the leaf and amongst shoots will result in differential photosynthetic rates within the seagrass canopy, thereby creating disparate water parcels with respect to TCO_2 on various spatial scales. In addition, the density of seagrass will result in different mixing rates and flow regimes that will further modify carbonate chemistry in time and space (Peterson et al. 2005, Koch et al. 2006, Marbà et al. 2006, Hendriks et al. 2014). The flow of water, TCO_2 concentration, and light, interact in a way that, together, determine carbon assimilation and uptake (McPherson et al. 2015), which directly affects the scale of seagrass OA mitigation. It is evident, then that spatial microzones of differential carbonate chemistry exist within the canopy of a seagrass bed. Interestingly, vulnerable calcifying organisms may exploit these microzones of refuge, as carbonate chemistry chemical cues have been shown to drive substrate selectivity for bivalves transitioning to the benthos (Green et al. 2013, Clements et al. 2016). This suggests that the importance of spatial carbonate chemistry heterogeneity is critical when predicting seagrass OA mitigation potential.

A multitude of other biological factors also determine the variability of carbonate chemistry within seagrass beds. Epiphytes growing on seagrass leaves can account for over 50% of the primary production in some seagrass meadows, however, the dominance of epiphytic photosynthesis over seagrass varies depending on the season (Thom 1990, Wear et al. 1999, Borowitzka et al. 2006). Epiphytic growth can vary dramatically depending on the morphology of seagrass—that is, small changes in morphology can lead to large changes in epiphytic assemblages (Borowitzka et al. 2006). The large percent of primary production by epiphytes is likely a dual component of reduced photosynthesis by seagrass leaves from epiphytic shading, and surface area abundance of algae epiphytic growth. Since our experiment did not include epiphytic photosynthesis as they were removed from our samples, it is necessary to understand and consider the contribution to, and role of, epiphyte primary production on carbonate chemistry when examining seagrass OA mitigation potential.

The variability in carbonate chemistry driven by biological cycling of CO_2 in seagrass beds is not just a result of shoot and epiphytic autotrophy, but by the significant contributions of carbon fixation via the microphytobenthos (Kaldy et al. 2002) and elevated rates of heterotrophic respiration fueled by high concentrations of organic matter retained within the canopy (Barrón et al. 2006 and references therein). In addition, seagrasses excrete small quantities of DOM into the water column and sediments stimulating heterotrophy, which in turn reduces net community production (Benner et a. 1986). Roots and rhizomes diffuse oxygen into the sediments, creating rich oxic layers that are exploited by benthic heterotrophs; the increased benthic respiration not only produces a positive flux of CO_2 out of the sediment, but also generates corrosive waters that actively dissolve the carbonate rich sediments associated with seagrasses (Marbà et al. 2006, Mazarrasa et al. 2015). Dissolution of carbonate sediments has a direct affect on the carbonate

system—that is, higher carbonate availability from $CaCO_3$ dissolution increases the buffering capacity of the system. Together, the myriad biological processes add substantial heterogeneity to the carbonate system within seagrass beds and, although, recent studies have quantified the ecosystem effect on the carbonate system as a whole (Manzello et al. 2012, Hendriks et al. 2014), the complexity of the system can hinder extrapolation to other seagrass systems in time and space.

Conclusions. A comparison of the photosynthetic potential between *Z. marina* and *Z. japonica* has implications for elucidating the contribution each species has on the carbonate system. In the higher intertidal zone where species overlap occurs, our results indicate that *Z. japonica* has a 3-fold greater photosynthetic potential than *Z. marina* when normalized to chlorophyll (Fig. 4). By measuring photosynthetic potential as a change in TCO_2, our findings could be extrapolated to estimate the predicted change in TCO_2 given measured mg chl gDW^{-1} and reported biomass m^{-2} in Padilla Bay (Bulthuis 2013) (Table 5, Fig. 9). *Z. japonica* appears to be better suited to mitigate OA on a per chlorophyll basis, given its higher photosynthetic rate and efficiency (Fig. 7 and 9). However, due to the 3:1 greater area covered by *Z. marina* over *Z. japonica* in Padilla Bay, *Z. marina* would have a 2.5x greater effect on carbonate chemistry when accounting for species total abundance. Additionally, our results indicate that *Z. japonica* stands to benefit more from moderate increases in TCO_2 by up regulating its photosynthetic potential (Fig. 5). The greater response of *Z. japonica* to TCO_2 may be a result of not only increased CO_2, but also increased HCO_3^- concentrations, whereas *Z. marina* appears to be saturated with respect to HCO_3^- (Fig 8a) (Invers et al. 2001). Due to the high variability within our treatments, any positive response to moderate increases in TCO_2 by *Z. marina* was likely obscured (Fig. 5, 8).

While a broader perspective of carbonate chemistry heterogeneity in time and space *in situ* will be needed when assessing potential seagrass OA mitigation, the photosynthetic potential of individual species with respect to not only irradiance and TCO_2, but temperature, salinity, and other environmental variables will need to be considered. This will become necessary when deciphering the favorable contributions each autotrophic group has on the carbonate system; particularly when two co-occurring seagrasses are in one specific region. Our results suggest that *Z. japonica* may increase its relative contribution to OA mitigation as TCO_2 rises in the coastal ocean. In addition, our study illuminates the potential of PNW populations of *Z. marina* and *Z. japonica* to modify the carbonate system, and provides a direct comparison of photosynthetic potential when exposed to varying levels of TCO_2. This is an initial step in attempting to determine the OA mitigation potential of seagrass systems in the PNW where a better understanding is needed (Blue ribbon panel on OA 2012). Further, our results could be integrated into larger scale biogeochemical models and observation networks aimed at deducing the individual contribution of seagrasses on reducing TCO_2, and the potential for creating areas of favorable carbonate chemistry (Khangaonkar et al. 2013, Alin et al. 2015).

References

Alin, S.R., Brainard, R.E., Price, N.N., Newton, J.A., Cohen, A., Peterson, W.T., DeCarlo, E.H., Shadwick, E.H., Noakes, S., Bednarsek, N., 2015. Characterizing the Natural System: Toward Sustained, Integrated Coastal Ocean Acidification Observing Networks to Facilitate Resource Management and Decision Support. Oceanography 28, 92–107. doi:10.5670/oceanog.2015.34

Backman, T., 1991. Genotypic and Phenotypic Variability of *Zostera marina* on the west coast of North America. Can. J. Bot.-Rev. Can. Bot. 69, 1361–1371.

Borowitzka, M.A., Lavery, P.S., van Keulen, M., 2006. Epiphytes of Seagrasses. In: Larkum, A.W.D., Orth, R.J., Duarte, C.M. (Eds.), Seagrasses: Biology, Ecology and Conservation. Springer, Dordrecht; London, pp. 441–461.

Barrón, C., Duarte, C.M., Frankignoulle, M., Borges, A.V., 2006. Organic carbon metabolism and carbonate dynamics in a Mediterranean seagrass (*Posidonia oceanica*) meadow. Estuaries Coasts 29, 417–426.

Barton, A., Hales, B., Waldbusser, G.G., Langdon, C., Feely, R.A., 2012. The Pacific oyster, *Crassostrea gigas*, shows negative correlation to naturally elevated carbon dioxide levels: Implications for near-term ocean acidification effects. Limnol. Oceanogr. 57, 698–710. doi:10.4319/lo.2012.57.3.0698

Beer, S., Koch, E., 1996. Photosynthesis of marine macroalgae and seagrasses in globally changing CO_2 environments. Mar. Ecol.-Prog. Ser. 141, 199–204. doi:10.3354/meps141199

Beer, S., Bjork, M., Hellblom, F., Axelsson, L., 2002. Inorganic carbon utilization in marine angiosperms (seagrasses). Funct. Plant Biol. 29, 349–354. doi:10.1071/PP01185

Beer, S., Rehnberg, J., 1997. The acquisition of inorganic carbon by the seagrass *Zostera marina*. Aquat. Bot. 56, 277–283. doi:10.1016/S0304-3770(96)01109-6

Bernhardt, J.R., Leslie, H.M., 2013. Resilience to Climate Change in Coastal Marine Ecosystems, in: Carlson, C.A., Giovannoni, S.J. (Eds.), Annual Review of Marine Science, Vol 5. Annual Reviews, Palo Alto, pp. 371–392.

Blue Ribbon Panel on Ocean Acidification, 2012. Ocean Acidification: From Knowledge to Action. 2012. Washington State's Strategic Response. Washington State Department of Ecology.

Bulthuis, Douglas A. 2013. The Ecology of Padilla Bay, Washington: An Estuarine Profile of a National Estuarine Research Reserve. Washington State Department of Ecology, Padilla Bay National Estuarine Research Reserve, Mount Vernon, WA, USA. 186 pp.

Cai, W.J., 2011. Estuarine and Coastal Ocean Carbon Paradox: CO_2 Sinks or Sites of Terrestrial Carbon Incineration?, in: Carlson, C.A., Giovannoni, S.J. (Eds.), Annual Review of Marine Science, Vol 3. Annual Reviews, Palo Alto, pp. 123–145.

Campbell, J.E., Fourqurean, J.W., 2013. Mechanisms of bicarbonate use influence the photosynthetic carbon dioxide sensitivity of tropical seagrasses. Limnol. Oceanogr. 58, 839–848. doi:10.4319/lo.2013.58.3.0839

Challener, R.C., Robbins, L.L., McClintock, J.B., 2016. Variability of the carbonate chemistry in a shallow, seagrass-dominated ecosystem: implications for ocean acidification experiments. Mar. Freshw. Res. 67, 163–172. doi:10.1071/MF14219

Chung, I.K., Beardall, J., Mehta, S., Sahoo, D., Stojkovic, S., 2011. Using marine macroalgae for

carbon sequestration: a critical appraisal. J. Appl. Phycol. 23, 877–886. doi:10.1007/s10811-010-9604-9

Ciais, P., C. Sabine, G. Bala, L. Bopp, V. Brovkin, J. Canadell, A. Chhabra, R. DeFries, J. Galloway, M. Heimann, C. Jones, C. Le Quéré, R.B. Myneni, S. Piao and P. Thornton, 2013: Carbon and Other Biogeochemical Cycles. In: Climate Change 2013: The Physical Science Basis. Contribution of Working Group I to the Fifth Assessment Report of the Intergovernmental Panel on Climate Change [Stocker, T.F., D. Qin, G.-K. Plattner, M. Tignor, S.K. Allen, J. Boschung, A. Nauels, Y. Xia, V. Bex and P.M. Midgley (eds.)]. Cambridge University Press, Cambridge, United Kingdom and New York, NY, USA, pp. 465–570, doi:10.1017/CBO9781107415324.015.

Clements, J.C., Woodard, K.D., Hunt, H.L., 2016. Porewater acidification alters the burrowing behavior and post-settlement dispersal of juvenile soft-shell clams (*Mya arenaria*). J. Exp. Mar. Biol. Ecol. 477, 103–111. doi:10.1016/j.jembe.2016.01.013

Cox, T.E., Gazeau, F., Alliouane, S., Hendriks, I.E., Mahacek, P., Le Fur, A., Gattuso, J.-P., 2016. Effects of in situ CO_2 enrichment on structural characteristics, photosynthesis, and growth of the Mediterranean seagrass *Posidonia oceanica*. Biogeosciences 13, 2179–2194. doi:10.5194/bg-13-2179-2016

Cummings, M.E., Zimmerman, R.C., 2003. Light harvesting and the package effect in the seagrasses *Thalassia testudinum* Banks ex König and *Zostera marina* L.: optical constraints on photoacclimation. Aquat. Bot. 75, 261–274. doi:10.1016/S0304-3770(02)00180-8

Dennison, W., Alberte, R., 1986. Photoadaptation and Growth of *Zostera marina* L. (eelgrass) Transplants Along a Depth Gradient. J. Exp. Mar. Biol. Ecol. 98, 265–282. doi:10.1016/0022-0981(86)90217-0

Dickson, A., Millero, F., 1987. A Comparison of the Equilibrium Constants for the Dissociation of Carbonic Acid in Seawater Media. Deep-Sea Research Part a-Oceanographic Research Papers 34, 1733–1743. doi:10.1016/0198-0149(87)90021-5

Doney, S.C., Fabry, V.J., Feely, R.A., Kleypas, J.A., 2009. Ocean Acidification: The Other CO_2 Problem. Annu. Rev. Mar. Sci. 1, 169–192. doi:10.1146/annurev.marine.010908.163834

Drake, L.A., Dobbs, F.C., Zimmerman, R.C., 2003. Effects of epiphyte load on optical properties and photosynthetic potential of the seagrasses *Thalassia testudinum* Banks ex König and *Zostera marina* L. Limnol. Oceanogr. 48, 456–463.

Duarte, C.M., Middelburg, J.J., Caraco, N., 2005. Major role of marine vegetation on the oceanic carbon cycle. Biogeosciences 2, 1–8.

Duarte, C.M., Marba, N., Gacia, E., Fourqurean, J.W., Beggins, J., Barron, C., Apostolaki, E.T., 2010. Seagrass community metabolism: Assessing the carbon sink capacity of seagrass meadows. Glob. Biogeochem. Cycle 24, GB4032. doi:10.1029/2010GB003793

Duarte, C.M., Hendriks, I.E., Moore, T.S., Olsen, Y.S., Steckbauer, A., Ramajo, L., Carstensen, J., Trotter, J.A., McCulloch, M., 2013. Is Ocean Acidification an Open-Ocean Syndrome? Understanding Anthropogenic Impacts on Seawater pH. Estuaries Coasts 36, 221–236. doi:10.1007/s12237-013-9594-3

Duffy, J.E., 2006. Biodiversity and the functioning of seagrass ecosystems. Mar. Ecol.-Prog. Ser. 311, 233–250. doi:10.3354/meps311233

Dumbauld, B.R., McCoy, L.M., 2015. Effect of oyster aquaculture on seagrass *Zostera marina* at the estuarine landscape scale in Willapa Bay, Washington (USA). Aquac. Environ. Interact. 7, 29–47. doi:10.3354/aei00131

Durako, M.J., Kunzelman, J.I., 2002. Photosynthetic characteristics of *Thalassia testudinum* measured in situ by pulse-amplitude modulated (PAM) fluorometry: methodological and scale-based considerations. Aquat. Bot. 73, 173–185. doi:10.1016/S0304-3770(02)00020-7

Ekstrom, J.A., Suatoni, L., Cooley, S.R., Pendleton, L.H., Waldbusser, G.G., Cinner, J.E., Ritter, J., Langdon, C., van Hooidonk, R., Gledhill, D., Wellman, K., Beck, M.W., Brander, L.M., Rittschof, D., Doherty, C., Edwards, P.E.T., Portela, R., 2015. Vulnerability and adaptation of US shellfisheries to ocean acidification. Nat. Clim. Chang. 5, 207–214. doi:10.1038/NCLIMATE2508

Enriquez, S., Merino, M., Iglesias-Prieto, R., 2002. Variations in the photosynthetic performance along the leaves of the tropical seagrass *Thalassia testudinum*. Mar. Biol. 140, 891–900. doi:10.1007/s00227-001-0760-y

Fassbender, A.J., Sabine, C.L., Feifel, K.M., 2016. Consideration of coastal carbonate chemistry in understanding biological calcification. Geophys. Res. Lett. 43, 2016GL068860. doi:10.1002/2016GL068860

Feely, R.A., Sabine, C.L., Hernandez-Ayon, J.M., Ianson, D., Hales, B., 2008. Evidence for upwelling of corrosive "acidified" water onto the continental shelf. Science 320, 1490–1492. doi:10.1126/science.1155676

Ferraro, S.P., Cole, F.A., 2012. Ecological periodic tables for benthic macrofaunal usage of estuarine habitats: Insights from a case study in Tillamook Bay, Oregon, USA. Estuar. Coast. Shelf Sci. 102, 70–83. doi:10.1016/j.ecss.2012.03.009

Fourqurean, J.W., Duarte, C.M., Kennedy, H., Marba, N., Holmer, M., Angel Mateo, M., Apostolaki, E.T., Kendrick, G.A., Krause-Jensen, D., McGlathery, K.J., Serrano, O., 2012. Seagrass ecosystems as a globally significant carbon stock. Nat. Geosci. 5, 505–509. doi:10.1038/ngeo1477

Gaylord, B., Kroeker, K.J., Sunday, J.M., Anderson, K.M., Barry, J.P., Brown, N.E., Connell, S.D., Dupont, S., Fabricius, K.E., Hall-Spencer, J.M., Klinger, T., Milazzo, M., Munday, P.L., Russell, B.D., Sanford, E., Schreiber, S.J., Thiyagarajan, V., Vaughan, M.L.H., Widdicombe, S., Harley, C.D.G., 2015. Ocean acidification through the lens of ecological theory. Ecology 96, 3–15. doi:10.1890/14-0802.1

Grantham, B.A., Chan, F., Nielsen, K.J., Fox, D.S., Barth, J.A., Huyer, A., Lubchenco, J., Menge, B.A., 2004. Upwelling-driven nearshore hypoxia signals ecosystem and oceanographic changes in the northeast Pacific. Nature 429, 749–754. doi:10.1038/nature02605

Green, M.A., Waldbusser, G.G., Hubazc, L., Cathcart, E., Hall, J., 2013. Carbonate Mineral Saturation State as the Recruitment Cue for Settling Bivalves in Marine Muds. Estuaries Coasts 36, 18–27. doi:10.1007/s12237-012-9549-0

Harris, K.E., DeGrandpre, M.D., Hales, B., 2013. Aragonite saturation state dynamics in a coastal upwelling zone. Geophys. Res. Lett. 40, 2720–2725. doi:10.1002/grl.50460

Harrison, P., 1982b. Comparative Growth of *Zostera japonica* Aschers. and Graebn. and *Zostera marina* L. Under Simulated Inter-Tidal and Subtidal Conditions. Aquat. Bot. 14, 373–379.

Harrison, P., Bigley, R., 1982a. The Recent Introduction of the Seagrass *Zostera japonica* Aschers. and Graebn. to the Pacific Coast of North-America. Can. J. Fish. Aquat. Sci. 39, 1642–1648.

Hauri, C., Gruber, N., McDonnell, A.M.P., Vogt, M., 2013. The intensity, duration, and severity

of low aragonite saturation state events on the California continental shelf. Geophys. Res. Lett. 40, 3424–3428. doi:10.1002/grl.50618
Hendriks, I.E., Olsen, Y.S., Ramajo, L., Basso, L., Steckbauer, A., Moore, T.S., Howard, J., Duarte, C.M., 2014. Photosynthetic activity buffers ocean acidification in seagrass meadows. Biogeosciences 11, 333–346. doi:10.5194/bg-11-333-2014
Hendriks, I.E., Duarte, C.M., Olsen, Y.S., Steckbauer, A., Ramajo, L., Moore, T.S., Trotter, J.A., McCulloch, M., 2015. Biological mechanisms supporting adaptation to ocean acidification in coastal ecosystems. Estuar. Coast. Shelf Sci. 152, A1–A8. doi:10.1016/j.ecss.2014.07.019
Hettinger, A., Sanford, E., Hill, T.M., Russell, A.D., Sato, K.N.S., Hoey, J., Forsch, M., Page, H.N., Gaylord, B., 2012. Persistent carry-over effects of planktonic exposure to ocean acidification in the Olympia oyster. Ecology 93, 2758–2768.
Hönisch, B., Ridgwell, A., Schmidt, D.N., Thomas, E., Gibbs, S.J., Sluijs, A., Zeebe, R., Kump, L., Martindale, R.C., Greene, S.E., Kiessling, W., Ries, J., Zachos, J.C., Royer, D.L., Barker, S., Marchitto, T.M., Moyer, R., Pelejero, C., Ziveri, P., Foster, G.L., Williams, B., 2012. The Geological Record of Ocean Acidification. Science 335, 1058–1063. doi:10.1126/science.1208277
Hofmann, G.E., Smith, J.E., Johnson, K.S., Send, U., Levin, L.A., Micheli, F., Paytan, A., Price, N.N., Peterson, B., Takeshita, Y., Matson, P.G., Crook, E.D., Kroeker, K.J., Gambi, M.C., Rivest, E.B., Frieder, C.A., Yu, P.C., Martz, T.R., 2011. High-Frequency Dynamics of Ocean pH: A Multi-Ecosystem Comparison. PLoS One 6, e28983. doi:10.1371/journal.pone.0028983
Invers, O., Zimmerman, R.C., Alberte, R.S., Perez, M., Romero, J., 2001. Inorganic carbon sources for seagrass photosynthesis: an experimental evaluation of bicarbonate use in species inhabiting temperate waters. J. Exp. Mar. Biol. Ecol. 265, 203–217. doi:10.1016/S0022-0981(01)00332-X
Jassby, A., Platt, T., 1976. Mathematical Formulation of Relationship Between Photosynthesis and Light for Phytoplankton. Limnol. Oceanogr. 21, 540–547.
Kaldy, J.E., Onuf, C.P., Eldridge, P.M., Cifuentes, L.A., 2002. Carbon budget for a subtropical seagrass dominated coastal lagoon: How important are seagrasses to total ecosystem net primary production? Estuaries 25, 528–539. doi:10.1007/BF02804888
Kaldy, J.E., 2006. Production ecology of the non-indigenous seagrass, dwarf eelgrass (*Zostera japonica* Ascher. & Graeb.), in a Pacific Northwest estuary, USA. Hydrobiologia 553, 201–217. doi:10.1007/s10750-005-5764-z
Kaldy, J.E., Shafer, D.J., Magoun, A.D., 2015. Duration of temperature exposure controls growth of *Zostera japonica*: Implications for zonation and colonization. J. Exp. Mar. Biol. Ecol. 464, 68–74.
Kenneth, A., Short, F.T., 2006. *Zostera*: Biology, Ecology, and Management. In: Larkum, A.W.D., Orth, R.J., Duarte, C. (Eds.), Seagrasses: Biology, Ecology and Conservation. Springer, Dordrecht; London, pp. 361–386.
Khangaonkar, T., Sackmann, B., Long, W., Mohamedali, T., Roberts, M., 2012. Simulation of annual biogeochemical cycles of nutrient balance, phytoplankton bloom(s), and DO in Puget Sound using an unstructured grid model. Ocean Dynamics 62, 1353–1379. doi:10.1007/s10236-012-0562-4
Koch, E.W., Ackerman, J., Verduin, J., van Keulen, M., 2006. Fluid Dynamics in Seagrass Ecology—from Molecules to Ecosystems. In: Larkum, A.W.D., Orth, R.J., Duarte, C.M.

(Eds.), Seagrasses: Biology, Ecology and Conservation. Springer, Dordrecht; London, pp. 193–225.
Koch, M., Bowes, G., Ross, C., Zhang, X.-H., 2013. Climate change and ocean acidification effects on seagrasses and marine macroalgae. Glob. Change Biol. 19, 103–132. doi:10.1111/j.1365-2486.2012.02791.x
Krause-Jensen, D., Duarte, C.M., Hendriks, I.E., Meire, L., Blicher, M.E., Marba, N., Sejr, M.K., 2015. Macroalgae contribute to nested mosaics of pH variability in a subarctic fjord. Biogeosciences 12, 4895–4911. doi:10.5194/bg-12-4895-2015
Kroeker, K.J., Kordas, R.L., Crim, R.N., Singh, G.G., 2010. Meta-analysis reveals negative yet variable effects of ocean acidification on marine organisms. Ecol. Lett. 13, 1419–1434. doi:10.1111/j.1461-0248.2010.01518.x
Kroeker, K.J., Kordas, R.L., Crim, R., Hendriks, I.E., Ramajo, L., Singh, G.S., Duarte, C.M., Gattuso, J.-P., 2013. Impacts of ocean acidification on marine organisms: quantifying sensitivities and interaction with warming. Glob. Change Biol. 19, 1884–1896. doi:10.1111/gcb.12179
Kurihara, H., 2008. Effects of CO_2-driven ocean acidification on the early developmental stages of invertebrates. Mar. Ecol.-Prog. Ser. 373, 275–284. doi:10.3354/meps07802
Larkum, A.W.D., Drew, E.A., Ralph, P.J., 2009. Photosynthesis and Metabolism in Seagrasses at the Cellular Level. In: Larkum, A.W.D., Orth, R.J., Duarte, C.M. (Eds.), Seagrasses: Biology, Ecology and Conservation. Springer, Dordrecht; London, pp. 323–345.
Lee, K.-S., Park, S.R., Kim, Y.K., 2007. Effects of irradiance, temperature, and nutrients on growth dynamics of seagrasses: A review. J. Exp. Mar. Biol. Ecol. 350, 144–175. doi:10.1016/j.jembe.2007.06.016
Leuschner, C., Rees, U., 1993. CO_2 Gas-Exchange of 2 Intertidal Seagrass Species, *Zostera-marina* L. and *Zostera-Noltii* Hornem During Emersion. Aquat. Bot. 45, 53–62. doi:10.1016/0304-3770(93)90052-X
Lorenzen, C.J., 1966. A method for the continuous measurement of in vivo chlorophyll concentration. Deep Sea Research and Oceanographic Abstracts 13, 223–227. doi:10.1016/0011-7471(66)91102-8
Love, B.A., O'Brien, C., Bohlmann, H., 2016. Photosynthetically Driven Cycles Produce Extreme pCO_2 variability in a Large Eelgrass Meadow and Readily Measured Proxies Can Be Used to Estimate These Changes., (EC54A–1311) presented at 2016 Ocean Sciences Meeting, AGU/ASLO/TOS, New Orleans, LA, 21–27 Feb.
Mach, M.E., Wyllie-Echeverria, S., Chan, K.M.A., 2014. Ecological effect of a nonnative seagrass spreading in the Northeast Pacific: A review of *Zostera japonica*. Ocean Coastal Manage. 102, 375–382. doi:10.1016/j.ocecoaman.2014.10.002
Major, K.M., Dunton, K.H., 2002. Variations in light-harvesting characteristics of the seagrass, *Thalassia testudinum*: evidence for photoacclimation. J. Exp. Mar. Biol. Ecol. 275, 173–189. doi:10.1016/S0022-0981(02)00212-5
Manzello, D.P., Enochs, I.C., Melo, N., Gledhill, D.K., Johns, E.M., 2012. Ocean Acidification Refugia of the Florida Reef Tract. PLOS ONE 7, e41715. doi:10.1371/journal.pone.0041715
Marbá, N., Holmer, M., Gacia, E., Barrón, C., 2006. Seagrass Beds and Coastal Biogeochemistry. In: Larkum, A.W.D., Orth, R.J., Duarte, C.M. (Eds.), Seagrasses: Biology, Ecology and Conservation. Springer, Dordrecht; London, pp. 135–157.
Marbá, N., Arias-Ortiz, A., Masque, P., Kendrick, G.A., Mazarrasa, I., Bastyan, G.R., Garcia-

Orellana, J., Duarte, C.M., 2015. Impact of seagrass loss and subsequent revegetation on carbon sequestration and stocks. J. Ecol. 103, 296–302. doi:10.1111/1365-2745.12370
Martin, S., Clavier, J., Guarini, J.M., Chauvaud, L., Hily, C., Grall, J., Thouzeau, G., Jean, F., Richard, J., 2005. Comparison of *Zostera marina* and maerl community metabolism. Aquat. Bot. 83, 161–174. doi:10.1016/j.aquabot.2005.06.002
Mateo, M.A., Renom, P., Hemminga, M.A., Peene, J., 2001. Measurement of seagrass production using the ^{13}C stable isotope compared with classical O_2 and ^{14}C methods. Mar. Ecol.-Prog. Ser. 223, 157–165. doi:10.3354/meps223157
Mazarrasa, I., Marba, N., Lovelock, C.E., Serrano, O., Lavery, P.S., Fourqurean, J.W., Kennedy, H., Mateo, M.A., Krause-Jensen, D., Steven, A.D.L., Duarte, C.M., 2015. Seagrass meadows as a globally significant carbonate reservoir. Biogeosciences 12, 4993–5003. doi:10.5194/bg-12-4993-2015
Mcleod, E., Chmura, G.L., Bouillon, S., Salm, R., Bjork, M., Duarte, C.M., Lovelock, C.E., Schlesinger, W.H., Silliman, B.R., 2011. A blueprint for blue carbon: toward an improved understanding of the role of vegetated coastal habitats in sequestering CO2. Front. Ecol. Environ. 9, 552–560. doi:10.1890/110004
McPherson, M.L., Zimmerman, R.C., Hill, V.J., 2015. Predicting carbon isotope discrimination in Eelgrass (*Zostera marina* L.) from the environmental parameters light, flow, and [DIC]. Limnol. Oceanogr. 60, 1875–1889. doi:10.1002/lno.10142
Mehrbach, C., Culberso.ch, Hawley, J., Pytkowic.rm, 1973. Measurement of Apparent Dissociation Constants of Carbonic Acid in Seawater at Atmospheric Pressure. Limnol. Oceanogr. 18, 897–907.
Onitsuka, T., Kimura, R., Ono, T., Takami, H., Nojiri, Y., 2014. Effects of ocean acidification on the early developmental stages of the horned turban, *Turbo cornutus*. Mar. Biol. 161, 1127–1138. doi:10.1007/s00227-014-2405-y
Orr, J.C., Fabry, V.J., Aumont, O., Bopp, L., Doney, S.C., Feely, R.A., Gnanadesikan, A., Gruber, N., Ishida, A., Joos, F., Key, R.M., Lindsay, K., Maier-Reimer, E., Matear, R., Monfray, P., Mouchet, A., Najjar, R.G., Plattner, G.K., Rodgers, K.B., Sabine, C.L., Sarmiento, J.L., Schlitzer, R., Slater, R.D., Totterdell, I.J., Weirig, M.F., Yamanaka, Y., Yool, A., 2005. Anthropogenic ocean acidification over the twenty-first century and its impact on calcifying organisms. Nature 437, 681–686. doi:10.1038/nature04095
Orth, R., Heck, K., Vanmontfrans, J., 1984. Faunal Communities in Seagrass Beds - a Review of the Influence of Plant Structure and Prey Characteristics on Predator Prey Relationships. Estuaries 7, 339–350. doi:10.2307/1351618
Oviatt, C., Rudnick, D., Keller, A., Sampou, P., Almquist, G., 1986. A Comparison of System (O_2 and CO_2) and ^{14}C Measurements of Metabolism. Mar. Ecol.-Prog. Ser. 28, 57–67. doi:10.3354/meps028057
Ow, Y.X., Uthicke, S., Collier, C.J., 2016. Light Levels Affect Carbon Utilisation in Tropical Seagrass under Ocean Acidification. PLoS One 11, e0150352. doi:10.1371/journal.pone.0150352
Palacios, S.L., Zimmerman, R.C., 2007. Response of eelgrass *Zostera marina* to CO_2 enrichment: possible impacts of climate change and potential for remediation of coastal habitats. Mar. Ecol.-Prog. Ser. 344, 1–13. doi:10.3354/meps07084
Peterson, C.H., Luettich, R.A., Micheli, F., Skilleter, G.A., 2004. Attenuation of water flow inside seagrass canopies of differing structure. Mar. Ecol.-Prog. Ser. 268, 81–92. doi:10.3354/meps268081

Pierrot, D., Lewis, E., and Wallace, D.W.R., 2006. MS Excel Program Developed for CO2 System Calculations. ORNL/CDIAC-105a. Carbon Dioxide Information Analysis Center, Oak Ridge National Laboratory, U.S. Department of Energy, Oak Ridge, Tennessee. doi: 10.3334/CDIAC/otg.CO2SYS_XLS_CDIAC105a

Pörtner, H.-O., 2008a. Ecosystem effects of ocean acidification in times of ocean warming: a physiologist's view. Mar. Ecol.-Prog. Ser. 373, 203–217. doi:10.3354/meps07768

Poppe, K. 2016. An Ecogeomorphic Model to Assess the Response of Padilla Bay 's Eelgrass Habitat to Sea Level Rise. Master's thesis, Western Washington Univ. Bellingham, WA, USA, unpublished.

Ruesink, J.L., Hong, J.-S., Wisehart, L., Hacker, S.D., Dumbauld, B.R., Hessing-Lewis, M., Trimble, A.C., 2010. Congener comparison of native (*Zostera marina*) and introduced (*Z. japonica*) eelgrass at multiple scales within a Pacific Northwest estuary. Biol. Invasions 12, 1773–1789. doi:10.1007/s10530-009-9588-z

Schwarz, A.M., Bjork, M., Buluda, T., Mtolera, H., Beer, S., 2000. Photosynthetic utilisation of carbon and light by two tropical seagrass species as measured in situ. Mar. Biol. 137, 755–761. doi:10.1007/s002270000433

Shafer, D.J., Kaldy, J.E., Sherman, T.D., Marko, K.M., 2011. Effects of salinity on photosynthesis and respiration of the seagrass *Zostera japonica*: A comparison of two established populations in North America. Aquat. Bot. 95, 214–220. doi:10.1016/j.aquabot.2011.06.003

Shafer, D.J., Kaldy, J.E., 2014. Comparison of photosynthetic characteristics of the seagrass congeners *Zostera marina* L. and *Zostera japonica* Ascher. & Graeb. Aquat. Bot. 112, 91–97. doi:10.1016/j.aquabot.2013.09.002

Shafer, D.J., Kaldy, J.E., Gaeckle, J.L., 2014. Science and Management of the Introduced Seagrass *Zostera japonica* in North America. Environ. Manage. 53, 147–162. doi:10.1007/s00267-013-0172-z

Silva, J., Sharon, Y., Santos, R., Beer, S., 2009. Measuring seagrass photosynthesis: methods and applications. Aquat. Biol. 7, 127–141. doi:10.3354/ab00173

Talmage, S.C., Gobler, C.J., 2009. The effects of elevated carbon dioxide concentrations on the metamorphosis, size, and survival of larval hard clams (*Mercenaria mercenaria*), bay scallops (*Argopecten irradians*), and Eastern oysters (*Crassostrea virginica*). Limnol. Oceanogr. 54, 2072–2080. doi:10.4319/lo.2009.54.6.2072

Thom, R., 1990. Spatial and Temporal Patterns in Plant Standing Stock and Primary Production in a Temperate Seagrass System. Bot. Marina 33, 497–510. doi:10.1515/botm.1990.33.6.497

Thom, R.M., 1996. CO2-Enrichment effects on eelgrass (*Zostera marina* L.) and bull kelp (*Nereocystis luetkeana* (MERT.) P. & R.). Water Air Soil Pollut 88, 383–391. doi:10.1007/BF00294113

Thom, R.M., Gaeckle, J.L., Buenau, K.E., Borde, A.B., Vavrinec, J., Aston, L., Woodruff, D.L., 2014. Eelgrass (*Zostera marina* L.) restoration in Puget Sound: Development and testing of tools for optimizing Site Selection. Pacific Northwest National Laboratory. United States Department of Energy, Oakridge, TN, USA. 351 pp.

Thomsen, J., Haynert, K., Wegner, K.M., Melzner, F., 2015. Impact of seawater carbonate chemistry on the calcification of marine bivalves. Biogeosciences 12, 4209–4220. doi:10.5194/bg-12-4209-2015

Unsworth, R.K.F., Collier, C.J., Henderson, G.M., McKenzie, L.J., 2012. Tropical seagrass

meadows modify seawater carbon chemistry: implications for coral reefs impacted by ocean acidification. Environ. Res. Lett. 7, 024026. doi:10.1088/1748-9326/7/2/024026
Waldbusser, G.G., Salisbury, J.E., 2014. Ocean Acidification in the Coastal Zone from an Organism's Perspective: Multiple System Parameters, Frequency Domains, and Habitats, in: Carlson, C.A., Giovannoni, S.J. (Eds.), Annual Review of Marine Science, Vol 6. Annual Reviews, Palo Alto, pp. 221–247.
Waldbusser, G.G., Hales, B., Langdon, C.J., Haley, B.A., Schrader, P., Brunner, E.L., Gray, M.W., Miller, C.A., Gimenez, I., 2015a. Saturation-state sensitivity of marine bivalve larvae to ocean acidification. Nat. Clim. Chang. 5, 273–280. doi:10.1038/NCLIMATE2479
Waldbusser, G.G., Hales, B., Langdon, C.J., Haley, B.A., Schrader, P., Brunner, E.L., Gray, M.W., Miller, C.A., Gimenez, I., Hutchinson, G., 2015b. Ocean Acidification Has Multiple Modes of Action on Bivalve Larvae. PLOS ONE 10, e0128376. doi:10.1371/journal.pone.0128376
Wallace, R.B., Baumann, H., Grear, J.S., Aller, R.C., Gobler, C.J., 2014. Coastal ocean acidification: The other eutrophication problem. Estuar. Coast. Shelf Sci. 148, 1–13. doi:10.1016/j.ecss.2014.05.027
Washington State Noxious Weed Control Board. 2012. Report of the Noxious Weed Control Board. Washington State Noxious Weed Control Board, Kent, WA, USA. pp. 28
Wear, D.J., Sullivan, M.J., Moore, A.D., Millie, D.F., 1999a. Effects of water-column enrichment on the production dynamics of three seagrass species and their epiphytic algae. Mar. Ecol.-Prog. Ser. 179, 201–213. doi:10.3354/meps179201
Wonham, M.J., Carlton, J.T., 2005. Trends in marine biological invasions at local and regional scales: the Northeast Pacific Ocean as a model system. Biol. Invasions 7, 369–392. doi:10.1007/s10530-004-2581-7
Zimmerman, R.C., Kohrs, D.G., Steller, D.L., Alberte, R.S., 1997. Impacts of CO_2 enrichment on productivity and light requirements of eelgrass. Plant Physiol. 115, 599–607.
Zimmerman, R.C., 2006. Light and Photosynthesis in Seagrass Meadows. In: Larkum, A.W.D., Orth, R.J., Duarte, C.M. (Eds.), Seagrasses: Biology, Ecology and Conservation. Springer, Dordrecht; London, pp. 303–321.

Appendix

A. Predicted photosynthetic parameters from hyperbolic tangent model (eq. 1) where P_{max} is the maximum photosynthetic rate, α is the photosynthetic efficiency, and R_d is the respiration rate normalized to gDW. Errors are 95% CI for individual parameters, and the root mean square error (RMSE) of the model fit. Trt. is the target PCO_2 treatment: 1, 2, 3, 4, 5 = 100, 250, 400, 800, and 1200 μatm, respectively.

Species	Target pCO_2.	Pmax	α	Rd	n	RMSE
Z. marina	100	187 ± 54	0.961 ± 0.69	21.8 ± 41	20	44.8
	250	236 ± 220	0.490 ± 0.85	20.7 ± 49	19	57.9
	400	214 ± 57	2.45 ± 1.9	−20.5 ± 49	20	48.9
	800	222 ± 74	1.16 ± 0.92	7.56 ± 49	20	57.3
	1200	220 ± 83	2.34 ± 2.3	−12.9 ± 94	20	72.1
Z. japonica	100	230 ± 67	2.00 ± 1.4	−28.6 ± 55	20	74.2
	250	292 ± 97	1.03 ± 0.85	−23.4 ± 55	17	143
	400	307 ± 156	1.47 ± 1.8	15.7 ± 101	18	152
	800	205 ± 118	6.79 ± 9.2	9.09 ± 101	19	216
	1200	319 ± 267	0.654 ± 1.0	38.9 ± 72	19	123

Units: P_{max} and R_d = μmol TCO_2 mg^{-1} chl h^{-1}; α = μmol TCO_2 mg^{-1} chl h^{-1} (μmol photons m^{-2} s^{-1})$^{-1}$

B. Summary of ANOVA results on respiration rates for *Z. marina* and *Z. japonica* across all pCO_2 treatments.

Source	Sum Sq.	d.f.	Mean sq.	F	Prob>F
Species	3939	1	3939	1.2	0.2814
pCO_2	25165	4	6291	1.92	0.1331
Spec*pCO_2	25958	4	6489	1.98	0.1233
Error	94833	29	3270	•	•
Total	154168	38	•	•	•

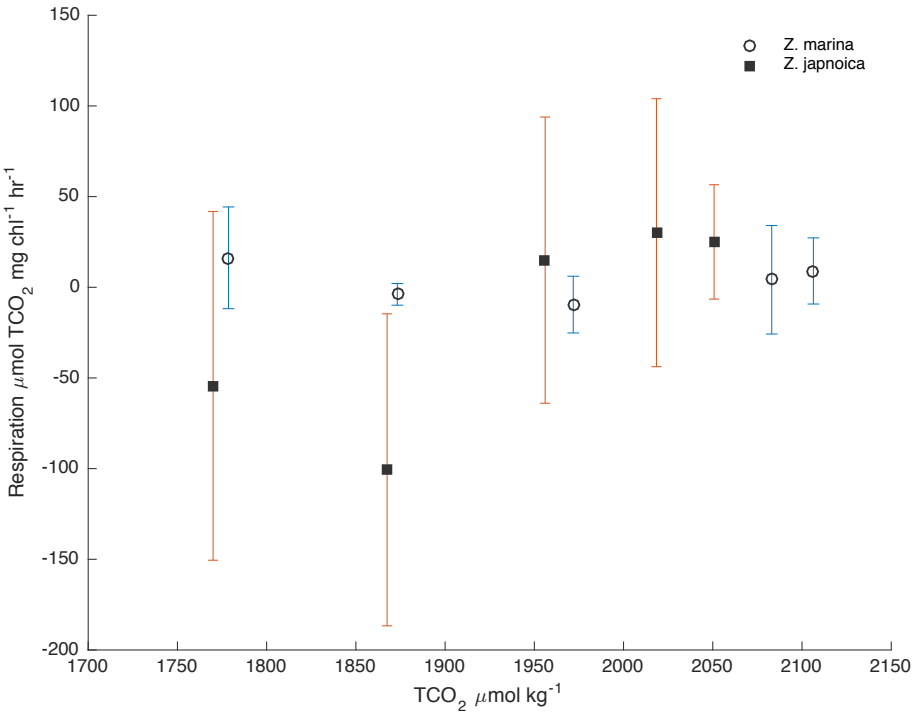

C. Respiration rates for *Z. marina* (open circles) and *Z. japonica* (closed squares) across all pCO_2 treatments.

D. ANOVA table from one-way analysis examining P_{max} values with main effect TCO_2.

Source	d.f.	Sum Sq	Mean Sq.	F-stat.	p-value
TCO_2	4	27094	6774	3.01	0.0258
Error	53	119078	2247	•	•
Total	57	146173	•	•	•